From Amsterdam and Mexico City to the World:
Heritage Conservation Areas in Comparative Perspective Pertaining to Water

David Leoni
7174667

A thesis submitted in partial fulfilment of the requirements for the degree of
MSc, Geographic Information Management & Applications (GIMA)

Responsible Professor: Ana Pereria Roders
Supervisor: Peter van Oosterom

May 28th, 2026

Abstract

This research presents a GIS-based comparative assessment of water-related risks to two UNESCO World Heritage Sites: the Amsterdam Canal Ring (WHS 1349, Netherlands) and the Historic Centre of Mexico City (WHS 412-001, Mexico), covering the period 2020 to 2025. A tiered analytical framework was developed combining globally consistent satellite-derived raster datasets (Tier 1) with city-specific local risk data sourced from national and municipal agencies (Tier 2). Tier 1 analysis applied zonal statistics across four global datasets, including JRC flood hazard, GMIS imperviousness, and JRC surface water occurrence, and seasonality, to four spatial zones defined by official UNESCO inscribed property boundaries. Tier 2 analysis integrated Amsterdam municipal flood probability and rainwater infiltration capacity data, EGMS Level 3 SAR-derived ground motion data, and Mexico City subsidence survey and waterlogging incident records, alongside heritage asset layers for both cities.

The Tier 1 analysis revealed that Amsterdam's heritage zone is excluded from the JRC global flood model due to its engineered flood defence infrastructure, while Mexico City's buffer zone records active modelled flood exposure with a mean depth of 0.68 metres under a 100-year return period scenario. Both sites exhibit high urban imperviousness with comparable mean values, though the risk implications differ substantially due to contrasting drainage contexts. The Tier 2 analysis identified subsurface mechanisms as the dominant risk at both sites: bidirectional groundwater dependency of 17th-century timber pile foundations at Amsterdam, and groundwater extraction-induced differential subsidence at rates of 92 to 115 mm/year at Mexico City. EGMS Level 3 data confirmed consistent low-magnitude subsidence across the Amsterdam heritage zone, with a mean velocity of -0.85 mm/year in the core zone. Spatial coincidence between high subsidence intensity zones and recurring waterlogging incidents at Mexico City is consistent with subsidence having disrupted urban drainage gradients, generating surface flooding as a secondary consequence of the primary groundwater risk.

The research demonstrates that global water-event related datasets systematically underestimate water risk at urban heritage sites and that the dominant risk mechanisms at both case study sites are invisible to surface remote sensing. A transferable, open-source tiered GIS workflow is presented as a replicable methodology for water risk assessment at World Heritage Sites, applicable wherever official inscribed boundaries and open spatial datasets are available. The findings support the integration of local contextual analysis into UNESCO State of Conservation monitoring as a necessary complement to global-scale assessment frameworks.

Statement on the Use of Gen-AI

Artificial intelligence tools were used in this thesis for limited support tasks, including text formatting, reference management, and improvements to Python code structure and logic. All research design, data processing, analysis, interpretation, and writing of substantive content were conducted independently by the author.

TABLE OF CONTENTS

GLOSSARY OF TERMS AND ACRONYMS

The following terms and acronyms are used throughout this thesis. Technical terms are defined as applied within the specific context of this research.

A. Acronyms and Abbreviations

Acronym	Full Term
AGEB	Area Geoestadistica Basica — Mexico's census unit, equivalent to a neighbourhood block, used as the spatial unit for CENAPRED vulnerability mapping
AHN	Actueel Hoogtebestand Nederland — the national detailed elevation dataset of the Netherlands
CENAPRED	Centro Nacional de Prevencion de Desastres — Mexico's national disaster prevention centre, publisher of the CDMX vulnerability datasets
CDMX	Ciudad de Mexico — the administrative designation for Mexico City
CRS	Coordinate Reference System — the mathematical framework defining how geographic coordinates relate to locations on the Earth's surface
DEM	Digital Elevation Model — a raster dataset representing the elevation of the land surface at a defined spatial resolution
EGMS	European Ground Motion Service — a Copernicus Land Monitoring Service product providing mean annual ground velocity measurements derived from Sentinel-1 SAR interferometry across Europe Note: Ground displacement as measured by EGMS is not itself a water hazard but is classified in this research as a hydrologically driven contextual indicator, as the primary drivers of ground motion in both study areas are water-related processes
GIS	Geographic Information System — software and methodological framework for capturing, storing, analysing, and visualising spatial data
GMIS	Global Man-made Impervious Surface — a 30m resolution Landsat-derived raster dataset measuring the percentage of sealed urban surface cover, produced by CIESIN/NASA SEDAC
gpkg	GeoPackage — an OGC standard file format for storing geospatial data, used for zonal statistics outputs in this research
InSAR / SAR	Interferometric Synthetic Aperture Radar — a remote sensing technique using radar satellite imagery to measure millimetre-scale surface deformation, including land subsidence
IPN	Instituto Politecnico Nacional — Mexico's national polytechnic institute, producer of the subsidence survey datasets used in the Tier 2 analysis
JRC	Joint Research Centre — the European Commission's science and knowledge service, producer of the global flood hazard and surface water datasets used in this research
NAP	Normaal Amsterdams Peil (Amsterdam Ordnance Datum) — the vertical reference datum used in the Netherlands, relative to which Amsterdam's below-sea-level elevations are measured
OSM	OpenStreetMap — a community-contributed global geographic database used as the source of heritage building and waterway vector data in this research
OUV	Outstanding Universal Value — the cultural or natural significance that is exceptionally important to present and future generations of humanity, constituting the basis for UNESCO World Heritage inscription (UNESCO World Heritage Centre, 2026)
QGIS	Quantum GIS — the open-source geographic information system software used for all spatial analysis in this research (version 3.22)
RS	Remote Sensing — acquiring Earth surface information from satellite or airborne sensors without direct contact
SGIRPC	Secretaria de Gestion Integral de Riesgos y Proteccion Civil — Mexico City's civil protection and risk management secretariat, publisher of the Atlas de Riesgos CDMX datasets
SoC	State of Conservation — the formal reporting mechanism through which UNESCO World Heritage States Parties document threats, management effectiveness, and conservation status of inscribed sites
SPC	Subprograma de Prevension y Contingencias — Mexico City risk prevention sub-programme, prefix used in the Atlas de Riesgos CDMX dataset naming convention
UNESCO	United Nations Educational, Scientific and Cultural Organisation — the UN agency responsible for the World Heritage Convention and the inscription and monitoring of World Heritage Sites
WH	World Heritage — used as an abbreviation for UNESCO World Heritage in the context of the World Heritage Convention
WHS	World Heritage Site — a site inscribed on the UNESCO World Heritage List under the World Heritage Convention (1972) as possessing Outstanding Universal Value

B. Key Technical Terms

Term	Definition as used in this research
Aquifer	A permeable geological formation that stores and transmits groundwater, used as the primary urban water supply source beneath Mexico.
Aquitard	A low-permeability geological layer that restricts vertical groundwater movement; the lacustrine clay beneath Mexico City functions as a compressible aquitard whose consolidation drives land subsidence.
Bidirectional groundwater risk	A condition where both elevated and depleted groundwater levels independently cause heritage damage, as in Amsterdam where rise causes moisture damage and depletion causes wooden pile decay.
Capillary moisture rise	Upward movement of water through masonry pores driven by surface tension, causing salt crystallisation and spalling of historic brick and plasterwork in Amsterdam canal houses.
Closed basin hydrology	A drainage condition where surface water and groundwater have no natural outlet to the sea or an external drainage network, causing precipitation and runoff to accumulate within the basin.
Differential subsidence	Spatially uneven land surface descent caused by heterogeneous lacustrine clay distribution, producing structural racking and drainage gradient disruption in Mexico City.
Fluvial flooding	Flooding caused by rivers or drainage channels overflowing their banks due to upstream precipitation, snowmelt, or hydrological shifts. Characterised by prolonged inundation and sediment transport.
Groundwater dependency	The reliance of a structure or ecosystem on a stable groundwater table for its physical integrity.
Imperviousness	The degree to which a land surface is sealed by impermeable materials (buildings, roads, paved areas), preventing rainfall infiltration into the soil.
Lacustrine clay	Fine-grained sedimentary deposits formed in ancient lake environments, characterised by high compressibility, low permeability, and extreme susceptibility to consolidation under load.
Majority (statistical)	The most frequently occurring value within a dataset or spatial zone, equivalent to the statistical mode. In zonal statistics, the majority identifies the dominant pixel value across a polygon zone.
Pluvial flooding	Flooding caused by intense rainfall overwhelming soil infiltration capacity and urban drainage systems, independent of river overflow. Particularly affects historic cities with high imperviousness and aging stormwater infrastructure.
Potentiometric level	The hydraulic pressure level of a confined aquifer; reduction through groundwater extraction initiates clay consolidation and land subsidence in Mexico City.
Polder	A low-lying area of land enclosed by embankments (dikes) and maintained below the surrounding water level through active pumping, characteristic of Dutch water management and the context within which the Amsterdam Canal Ring WHS is situated.
Raster	A spatial data format representing geographic information as a regular grid of cells (pixels), each containing a single numerical value. All global risk datasets used in the Tier 1 analysis are raster format.
State of Conservation (SoC)	The formal UNESCO reporting mechanism through which World Heritage States Parties document the conservation status of inscribed sites, including the identification of threats to OUV. SoC reports form a primary source for global assessments of heritage water risk.
Subsidence	The gradual sinking or settling of the ground surface.
Tier 1 analysis	The global comparative analysis tier of this research, employing standardised, globally consistent raster datasets applied identically to both Amsterdam and Mexico City, enabling direct quantitative comparison.
Tier 2 analysis	The local contextual analysis tier of this research, employing city-specific datasets sourced from national and municipal agencies, providing site-specific risk profiles beyond the resolution of global datasets.
Waterlogging	Accumulation of surface water following intense rainfall that exceeds urban drainage capacity, causing temporary ponding independent of river or canal overflow.
WHS buffer zone	A spatially defined outer zone surrounding the WHS core boundary, used to assess risk conditions in the immediate heritage setting.
WHS core zone	The precisely inscribed boundary of a World Heritage Site as defined in the nomination dossier and maintained by the UNESCO World Heritage Centre, representing the area of primary Outstanding Universal Value.
Zonal statistics	A GIS operation extracting and summarising raster pixel values within a vector polygon, producing mean, minimum, maximum, and majority statistics per zone.

1. INTRODUCTION

1.1 Background

Human settlements require a continuous evolution in their management methods of World Heritage (WH) sites to support WH sustainability and conserve their outstanding universal value (OUV). OUV is a term that describes cultural or natural significance that is exceptionally important to present and future generations of humanity, thus requiring heritage protection (UNESCO World Heritage Centre, 2026). This research will investigate the State of Conservation (SoC) of WH by understanding the distinct threats to OUV.

Effective conservation of World Heritage Sites (WHS) increasingly depends on the capacity to monitor risks systematically and continuously, particularly those related to water. Water-driven hazards such as flooding, erosion, groundwater rise, and hydrological instability are dynamic processes that evolve alongside climate change, urbanization, and environmental degradation. Without structured monitoring, these changes often remain undetected until they cause irreversible damage to the Outstanding Universal Value (OUV) of a site. Risk monitoring provides an evidence-based foundation for conservation by identifying emerging threats early, revealing spatial patterns of vulnerability, and enabling heritage managers to prioritize interventions before deterioration accelerates. It also strengthens the SoC reporting process by supplying consistent, spatially explicit information that can be compared over time. In this way, risk monitoring is not only a diagnostic tool but a strategic component of long-term heritage governance, ensuring that conservation decisions are informed, proactive, and aligned with the evolving environmental realities facing both cultural and natural heritage.

This research will globally analyze the distinct threats that pertain to water impacting the SoC of two (2) select cultural World Heritage sites. Water-related threats include pluvial flooding, pluvial flooding, coastal flooding and sea level rise, groundwater rise, groundwater depletion, land subsidence (groundwater extraction-induced), erosion and sediment transport, waterlogging, drought-induced moisture stress, water quality degradation and pollution, and hydrological regime change.

The focus of this research includes a *comparative analysis* with Amsterdam and Mexico City to identify water-related risks in a comparative perspective considering the varying urban landscapes and hydrologic systems (and their intersectionality) of the two cities. Furthermore, to account for differences in data availability between the two cities, individual *local spatial analyses* will be performed. This approach enables the use of local datasets and supports additional analytical findings from data that do not overlap across both WH sites. The analysis will be conducted using GIS-based approaches, including remote sensing and multi-variate spatial analysis.

1.2 Research Scope

The overarching objective of this research is to develop a workflow for a GIS-based evaluation of water-related events that contribute risk to two (2) UNESCO World Heritage sites within the period of 2020-2025, and to analyze the impact of human settlement to inform more effective conservation and management strategies.

To achieve this general objective, the research will address the following sub-objectives and corresponding research questions:

Research Question 1
What are the prevalent water-related threats impacting World Heritage sites globally between 2020 and 2025?

Research Question 2
What are the specific threats to natural heritage from water, and how do their behaviours distinctly impact the Outstanding Universal Value of these sites?

Research Question 3
What are the specific threats to cultural heritage from water, and how do their behaviours distinctly impact the OUV of these sites?

Research Question 4
How do the spatial and cultural dynamics of human settlements (e.g., urbanization, land-use changes, socio-economic factors) exacerbate or mitigate water threats to World Heritage in both cultural and natural heritage contexts?

Research Question 5
How can GIS-based approaches, combined with quantitative and qualitative methods, be effectively utilized to assess water-related hazards, exposure, and vulnerability, thereby improving the conservation, sustainability, and overall management of WH sites?

Research Question 6
What remote sensing capabilities are most effective for local-level assessment, monitoring, and mitigation of water threats to World Heritage, and how can they be integrated into GIS frameworks?

1.3 Scope and Limitations

This research will focus exclusively on water-related events and their impacts on World Heritage sites, within the 2020-2025 timeframe. Snow-related hazards are excluded unless snowmelt processes directly contribute to hydrological risk. It will not research other categories of climate-induced threats (e.g., wildfires, extreme heat, unless directly linked to water cycles). While the study will employ a global lens for threat identification, the in-depth GIS analysis and associated research questions will be applied to selected case study cities and sites, rather than attempting a comprehensive site-by-site global assessment. The study will not conduct primary data collection through fieldwork but will rely on existing scientific data, remote sensing products, and academic literature. Furthermore, while the research aims to inform conservation strategies, it will not develop detailed engineering or policy solutions but will rather provide a scientific basis for their formulation. The primary objective is evaluation and understanding, not implementation.

UNESCO assigns each World Heritage Site a unique identification code, and multi-component properties receive sub-unit numbers to distinguish their individual inscribed areas. WHS 412 therefore consists of two components: the Historic Centre of Mexico City (WHS 412-001) and Xochimilco (WHS 412-002). WHS 412 is jointly inscribed with Xochimilco (WHS 412-002), which was explicitly excluded from this analysis. The Xochimilco wetland system retains active surface water directly detectable by the raster datasets utilized in this research. A complete water-risk assessment of WHS 412 would require analysis of both inscribed components. The exclusion of Xochimilco is acknowledged as a scope limitation and its inclusion is recommended as a priority for future research, addressed further in Section 7.1. The Seventeenth-Century Canal Ring of Amsterdam (WHS 1349) is examined in parallel as the second case study city of this research.

2. LITERATURE REVIEW

2.1 Global Water Events (2020-2025)

Between 2020 and 2025, global assessments of World Heritage vulnerability have increasingly emphasized the accelerating influence of water-related hazards. Across multiple large-scale studies, including UNESCO State of Conservation (SoC) reports, continental hazard rankings, and global multi-risk analyses, water emerges as one of the most pervasive and rapidly intensifying drivers of degradation to both cultural and natural heritage. Systematic reviews of SoC reports from 1979-2021 show that climate change and severe weather has become the dominant threat category, with recent trends indicating a shift from slow-onset processes such as sea-level rise toward more frequent and extreme hydrological events (Nguyen and Baker, 2023).

A central component of these water-related risks is the increasing prevalence of pluvial and fluvial flooding, two hydrological processes that affect heritage in distinct ways. Pluvial flooding results from intense rainfall overwhelming soil infiltration and urban drainage systems, disproportionately affecting historic cities where impermeable surfaces and aging stormwater networks heighten vulnerability (Ginzarly et al., 2024). Fluvial flooding, by contrast, occurs when rivers and drainage channels overflow due to upstream precipitation, snowmelt, or hydrological shifts. These events can cause prolonged inundation, sediment transport, and structural destabilization, particularly in natural heritage landscapes (Arrighi, 2021). Globally, approximately 35% of natural sites and 21% of cultural and mixed sites are currently exposed to riverine flood hazards (Arrighi, 2021). Figure 1 illustrates this distribution through a global flood-risk classification, derived from hydrological exposure and the vulnerability of site-specific conditions.

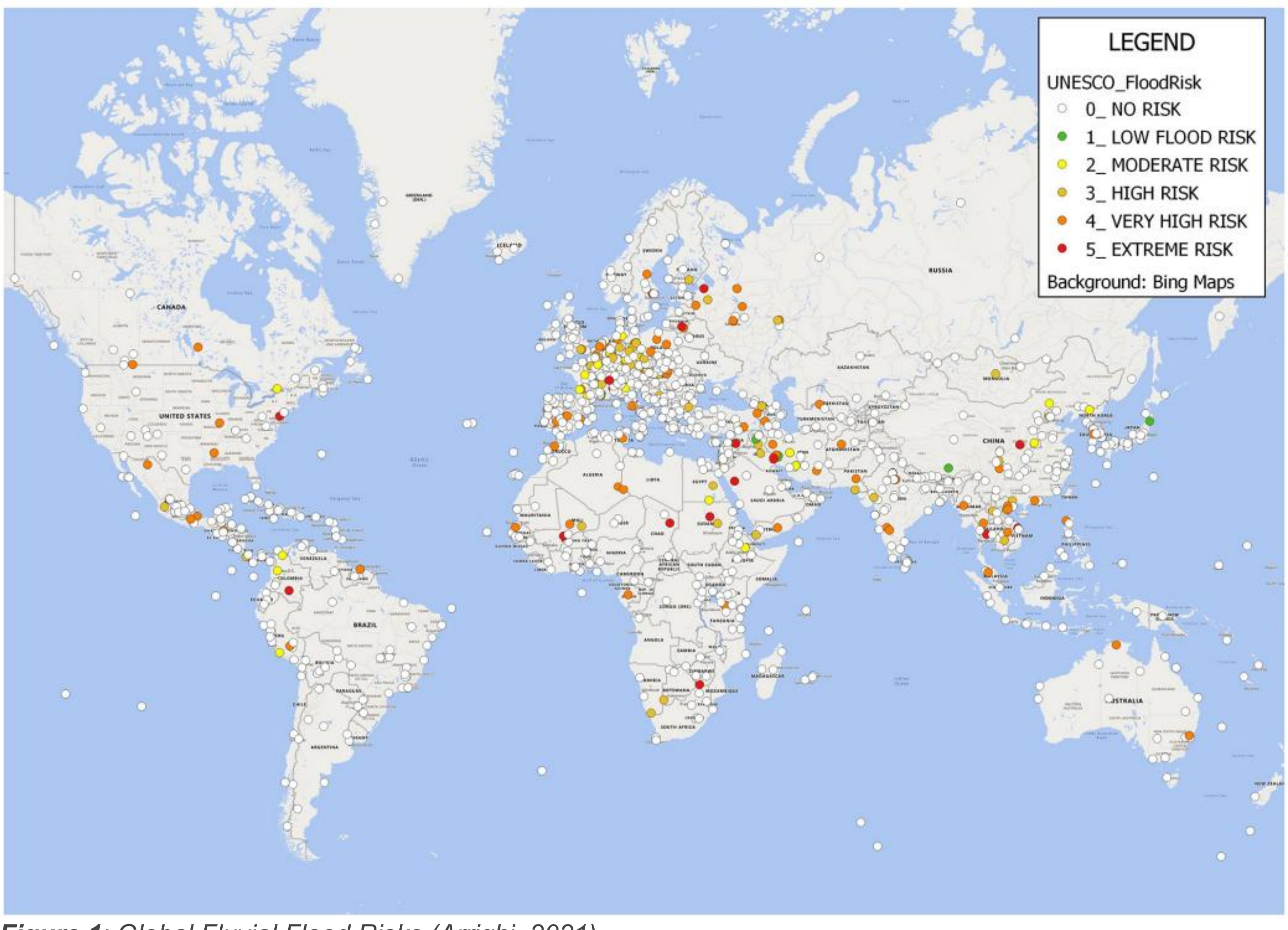

***Figure 1**: Global Fluvial Flood Risks (Arrighi, 2021)*

Similarly, Li (2024) surveyed 48 World Heritage properties across 41 countries (primarily in Europe and Asia) and concluded that water-related risks such as floods, storms, landslides, erosion, and sea-level rise were among the most frequently reported pressures on Outstanding Universal Value (OUV). This data is displayed in Figure 2.

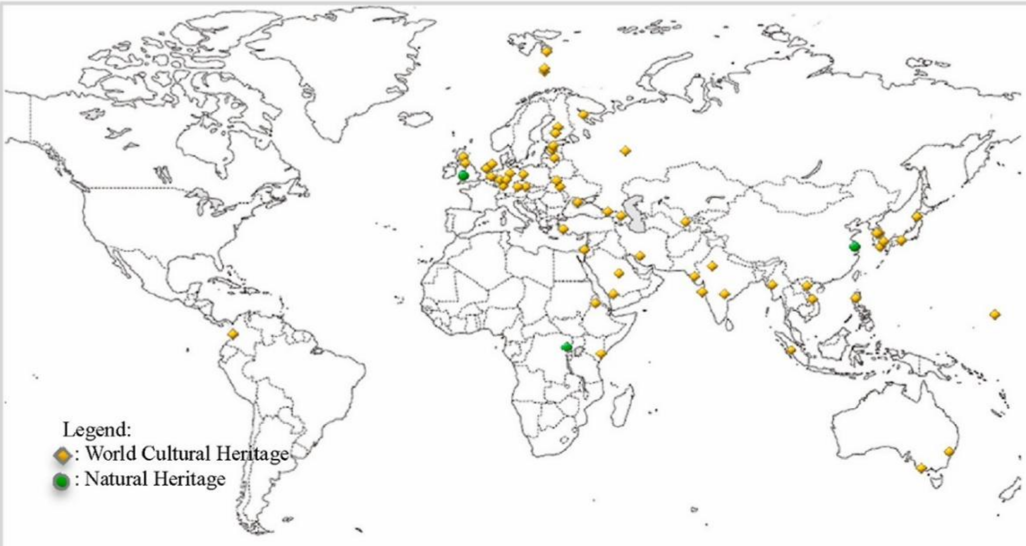

(Number of sites)	Cultural heritage (number of sites)				Natural heritage	Total
	Monuments	Groups of buildings	Cultural landscapes	Archaeological sites (remains, or relics)		
Asia	1	**8**	1	**6**	1	**17**
Pacific Ocean	0	0	0	1	0	1
Europe	2	**12**	1	**4**	1	**20**
South America	0	0	1	0	0	1
Middle East	0	0	1	3	0	4
Africa	0	1	0	0	1	2
Oceania	0	2	1	0	0	3
Total	3	**23**	5	**14**	3	48

Fire	Earthquake	Flood	Storm	Landslide	Tsunami	Riverbank/coastal erosion	Sea level rise	Extreme weather events	Pollution	Armed conflict	Vandalism/theft	Terrorism
33	**25**	**29**	**15**	**11**	4	8	5	7	10	5	**18**	8
68.8%	**52.1%**	**60.4%**	**31.3%**	**22.9%**	8.3%	16.7%	10.4%	14.6%	20.8%	10.4%	**37.5%**	16.7%

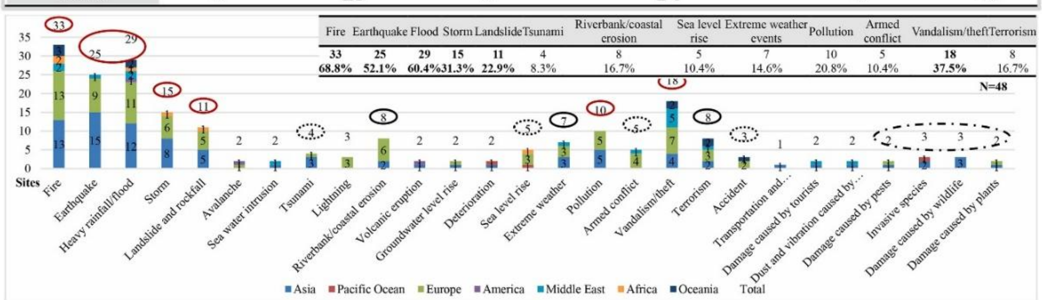

***Figure 2**: Global Risks to World Heritage (Li, 2024)*

However, Li's dataset is inherently shaped by the geographic distribution of available management plans: 77% of the surveyed sites are located in Europe and Asia, resulting in a sample that reflects the hazard profiles of these continents more strongly than those of Africa, the Arab States, or Latin America. Within this Euro-Asian concentration, hydrological hazards appear prominently; 60.4% of sites reported flood impacts, and 16.7% reported riverbank or coastal erosion. This indicates that water-related events are consistently embedded in the disaster histories and management concerns of these regions. While the study provides valuable insight into the types of water hazards affecting heritage, its continental bias means that global patterns are only partially represented, with under-reported water risks in regions where management plans are less frequently published or less detailed.

The IUCN World Heritage Outlook 4 (Aylett et al., 2025) provides the most comprehensive global assessment of the conservation status of all natural and mixed UNESCO World Heritage sites. Utilizing four assessment cycles (2014, 2017, 2020, 2025), the report evaluates each site's SoC, the severity of current and potential events, and the effectiveness of protection and management systems. A central finding is that climate change has become the most prevalent and fastest-growing threat, surpassing invasive species and tourism pressures. The report highlights that more sites have deteriorated than improved since 2017, with only half of all natural sites demonstrating effective management. It is also important to note that within the category Climate Change and Severe Weather, the following sub-threats are contained within the category: changes in physical and chemical regimes, changes in temperature regimes, and changes in precipitation and hydrological regime. Thus, this category is not fully encompassing of solely water-related threats.

Figure 3 depicts the number of natural WHS affected by different events in 2014, 2017, 2020, and 2025. An upward trend across nearly all threat categories demonstrates increasing threat over time. Climate change and severe weather show the most dramatic increase, followed by invasive species, recreational activities, and hunting and fishing pressures. The water-related events that are defined in this classification include: climate change and severe weather, water-borne and other effluent pollution, dams and water management, and wastewater events.

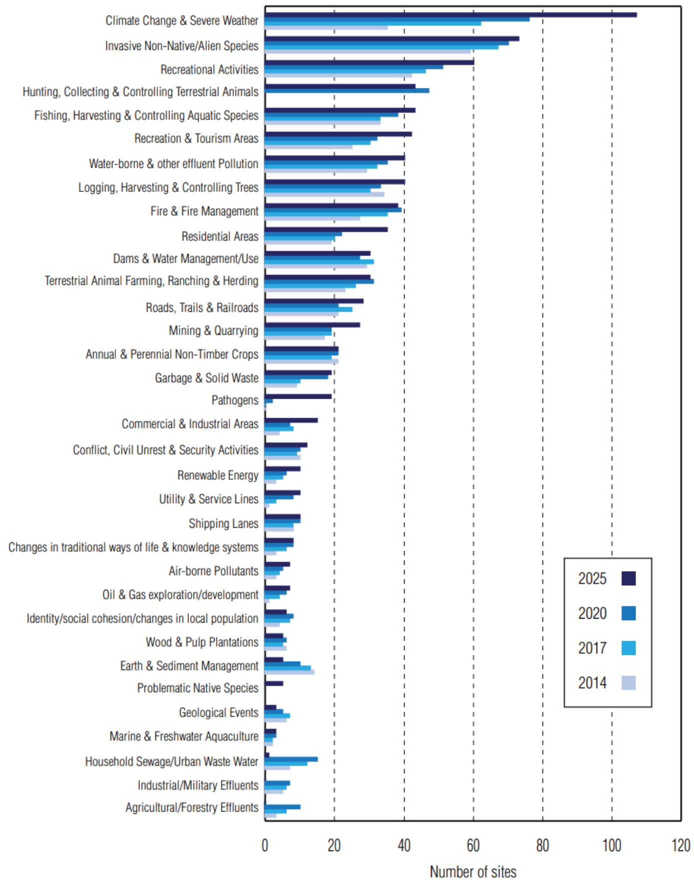

Complementing these global analyses, continental-scale studies provide additional insight into water-related events that may impact WH. The multi-risk analysis on European cultural and natural UNESCO heritage sites (Valagussa et al., 2021) identified water events including flooding, storms, erosion, and oceanic water changes as key threats affecting both cultural and natural WHS. Figure 4 presents the results of the hazard ranking.

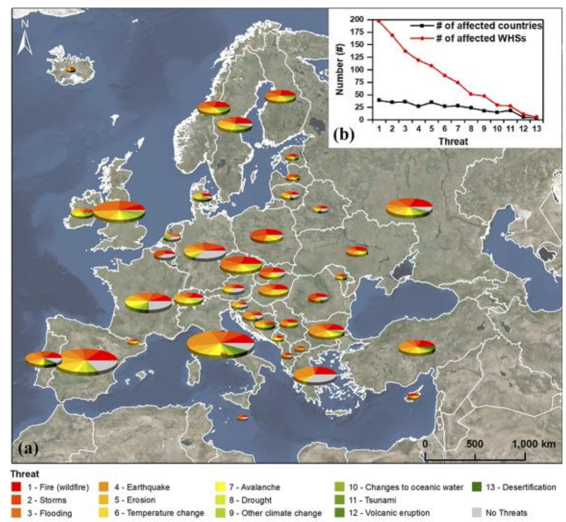

Note(s): The size of the pie charts is a function of how many times the threats affect the WHSs of each country and the number of sites without threats

Figure 4: *Threats to World Heritage in Europe (Valagussa et al., 2021)* ***Figure 3****: Global Risks to WH (Aylett et al., 2025)*

Overall, these research findings provide valuable insights into assessing and understanding the risks to WHS that are related to water. Extreme weather events including storms, alongside broader shifts in the greater hydrologic cycle, erosion, and water management pressures, collectively signal a global intensification of water-driven threats.

2.2 Cultural vs Natural Heritage Vulnerability

Specific threats may interact with natural versus cultural heritage sites in a different dynamic. For example, natural heritage sites often cover vast spatial extents, making them highly susceptible to river flood transport of contaminants and ecosystem disruption (Arrighi, 2021). Cultural heritage vulnerabilities are determined by material science and urban density. The urban fabric, including building age, material porosity, and proximity to water, dictates the damage valuation (Ginzarly et al., 2024). Cultural heritage is also susceptible to intangible loss, where water hazards may interrupt the social practices, knowledge transmission, and community systems that sustain a site (Ginzarly et al., 2024). When people can no longer perform or transmit practices, the living value of the site may degrade even if the physical cultural fabric survives.

2.3 Human Settlements and Urban Fabric Dynamics

Human settlements play a central role in shaping the vulnerability of World Heritage Sites (WHS), particularly as urbanization accelerates and land-use pressures intensify. A global survey of human settlements managing World Heritage (Pereira Roders et al., 2015) demonstrates that approximately two-thirds of all cultural and mixed properties (571 sites) are managed by 1,631 human settlements. This number has grown exponentially since 2009. This expansion reflects not only the increasing number of WHS but also the growing complexity of their management, as many properties now involve multiple settlements, serial nominations, or cultural landscapes.

The nature of how OUV is materialized within a settlement directly determines the structure of heritage governance and, by extension, the capacity to monitor and respond to water-related events. Pereira Roders (2010) proposes a classification of World Heritage cities according to two principal variables: character, distinguishing between individual properties managed by a single settlement and collective properties whose OUV is shared across multiple settlements; and consistency, describing how the OUV is distributed across buildings and locations within the settlement. This framework generates eight categories (A1 through A4 for individual, B1 through B4 for collective) ranging from singular OUV concentrated in one building to absolute OUV covering an entire urban area.

This classification has direct implications for water risk management. Amsterdam (WHS 1349) corresponds to Category A3 - Individual, Consolidated: the OUV is materialized in varied buildings across one concentrated location within one urban settlement, the 17th-century canal ring, managed by a single municipal authority with clearly defined spatial boundaries. This consolidated management structure enables the sophisticated, integrated water risk governance reflected in the Climate Flood Hazard (Klimaateffectatlas) flood model and the Amsterdam Rainproof programme, both products of a single accountable municipal body. Mexico City (WHS 412) corresponds to Category A2 - Individual, Fragmented: the OUV is fragmented across varied buildings in varied locations within one urban settlement, and the joint inscription with Xochimilco further distributes management responsibility. Pereira Roders (2010) explicitly cites Mexico City as an example of the fragmented category. The resulting governance fragmentation, with multiple national and municipal agencies holding partial jurisdiction over different components of the heritage zone, directly contributes to the heterogeneous, multi-source data landscape encountered in Chapter 3 and to the observed gaps in coordinated water-related event monitoring for the site.

The shift from singular, monument-based inscriptions toward shared Outstanding Universal Value (OUV) and large cultural landscapes has increased the number of settlements responsible for managing conservation areas. As a result, WHS are increasingly embedded within dense, evolving urban environments where pressures from housing, infrastructure, tourism development, and land conversion intersect with environmental hazards. This spatial entanglement heightens exposure to water-related risks, as many settlements are located along rivers, coasts, or low-lying terrain where hydrological processes and urban expansion converge.

Recent spatiotemporal analyses reinforce this trend. Katontoka et al. (2024) examined built-up area growth across 668 cultural WHS between 1985 and 2015 and found that urban densification is widespread, even in properties that do not report urban development as a threat in their State of Conservation (SoC) reports, suggesting a gap between on-the-ground urban transformation and official monitoring.

These findings have direct implications for water-related risks. Urban densification alters drainage patterns, increases impervious surfaces, and amplifies runoff, thereby intensifying pluvial flooding and exacerbating the impacts of extreme rainfall events. In historic cities, densification can strain aging stormwater systems, while in natural or mixed sites, expanding settlements can encroach on floodplains, wetlands, and buffer zones that historically mitigated hydrological hazards. Moreover, the uneven distribution of reporting, where Europe and Asia dominate SoC submissions, creates a geographical bias in global datasets, obscuring water-related vulnerabilities in regions where reporting is less frequent or less detailed. Understanding these settlement patterns is therefore essential for interpreting global water-related events and for developing risk assessments that reflect the lived realities of heritage sites embedded within rapidly changing urban landscapes.

2.4 GIS and Remote Sensing in Heritage Science

Modern conservation relies on Earth Observation to bridge the gap between global monitoring and local action. Studies which utilize Earth datasets are integral to understanding the unique spatial dynamics between human settlements, world heritage sites, and their risk mechanisms. A Global Scale Analysis of River Flood Risk of UNESCO World Heritage Sites (Arrighi, 2021) utilizes global river flood hazard data from the Joint Research Center (JRC) of the Copernicus initiative of the European Commission, openly available at the JRC Data Catalog (https://data.jrc.ec.europa.eu/). These raster datasets provide scientific insights into the assessment of changing threat exposures which can be incorporated into any threat analysis.

Remote sensing also supports long-term monitoring of settlement expansion, which indirectly shapes water risk. Katontoka et al. (2024) use the World Settlement Footprint Evolution (WSF-Ev) dataset, an annual 30m raster of global built-up area from 1985-2015, to quantify densification within WHS core zones. Although focused on urbanization, these findings highlight how expanding impervious surfaces intensify pluvial flooding and alter hydrological regimes, reinforcing the need to integrate settlement dynamics into water-risk assessments.

3. METHODOLOGY

3.1 Overview of Methods

This research designs and develops a GIS/RS workflow to evaluate water-related risks to UNESCO World Heritage Sites (WHS) between 2020 and 2025. The methodology of this GIS workflow follows a tiered analytical framework, beginning with a quantitative *global comparative assessment* of water-related events across both case study cities using globally available raster datasets and zonal statistics within the boundaries of WH. This is followed by a *local-level spatial analysis* of Amsterdam (WHS 1349) and the Historic Centre of Mexico City (WHS 412-001), drawing on distinct national and municipal datasets available in each country. The global tier establishes a consistent comparative baseline, while the local tier enables finer-scale, context-specific analysis. Detailed analytical procedures are described in Section 3.6.

Although WHS 412 comprises two jointly inscribed components: the Historic Centre (412-001) and Xochimilco (412-002), this research focuses exclusively on the Historic Centre component. Xochimilco is referenced contextually where relevant to understand the broader lacustrine heritage landscape but is not included in the primary spatial analysis. All spatial analysis was conducted using QGIS 3.22, with data processing and batch zonal statistics executed via a custom Python script within the QGIS Python console. The coordinate reference system adopted throughout is WGS84 (EPSG:4326), with city-specific coordinate systems applied where local datasets required.

3.2 Tiered Analytical Framework

A two-tier analytical framework (Figure 5) was developed to enable the use of all available data sources for assessing and spatially visualizing water-related risks. The global tier supports true comparative analysis through the application of standardized satellite datasets, which allow for consistent quantitative operations such as zonal statistics across both cities. The local tier incorporates national and municipal heritage and environmental datasets that, by design, are specific to each country's heritage management system and therefore cannot be used for direct cross-city comparison.

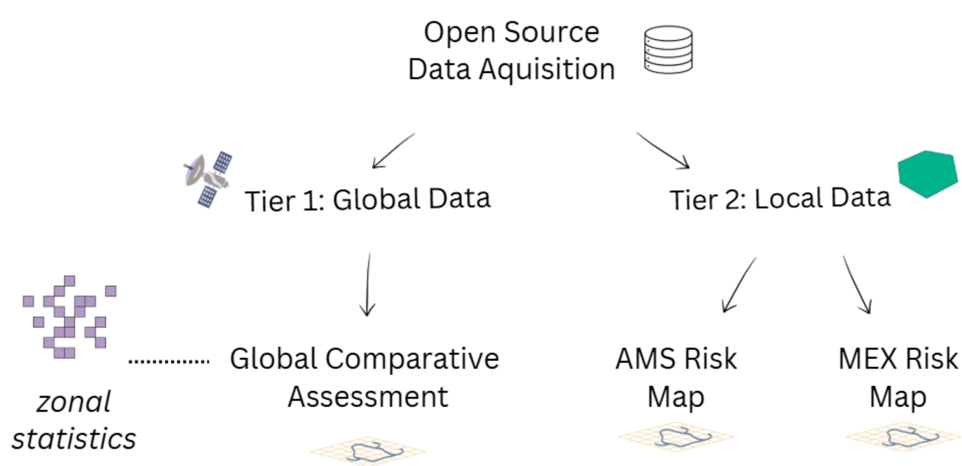

***Figure 5**: Tiered Analytical Framework Schema*

Tier 1 constitutes the global comparative analysis, employing standardized, globally consistent raster datasets applied identically across both case study sites. This tier enables direct quantitative comparison between Amsterdam and Mexico City and addresses Research Questions 1, 2, 3, and 4. Tier 2 constitutes the local contextual analysis, utilizing city-specific datasets sourced from national and municipal agencies in the Netherlands and Mexico. Although these datasets are not designed for cross-national comparability, they are analyzed in parallel to generate site-specific risk profiles that reveal localized water-related events not captured by global datasets alone. This tier addresses Research Questions 4, 5, and 6.

3.3 Case Study Selection

Amsterdam and Mexico City were selected as comparative case studies to examine how water-related evemts manifest across contrasting World Heritage urban settlements. Both cities face significant hydrological pressures, yet their underlying drivers, settlement morphologies, heritage typologies, and hydrological characters differ fundamentally, making comparison analytically productive. Amsterdam represents a hydrologically engineered, low-lying European canal city where water management is embedded in its cultural identity and physical infrastructure. Mexico City, by contrast, is a rapidly urbanising metropolis situated on a former lakebed, where groundwater extraction, pluvial flooding, and differential land subsidence create complex and evolving water risks. By analysing these two cities through a consistent GIS-based workflow, the study captures a spectrum of water-related vulnerabilities across both cultural heritage typologies and urban water management contexts.

3.4 Heritage Boundary Delineation

For Amsterdam, both the WHS core zone and outer heritage zone boundaries were sourced from the UNESCO World Heritage Cities Programme ArcGIS Feature Service (UNESCO Urban Heritage Atlas, 2025). Specifically, two dedicated inscribed property layers were used: the Inscribed_property_amsterdam_canaldistrict layer (Feature Service layer 5) as the WHS core zone, and the Inscribed_property_amsterdam_bufferzone layer (Feature Service layer 6) as the outer heritage zone. These layers represent the officially inscribed WHS 1349 boundary (see Appendix A) and its designated buffer zone as maintained by the UNESCO World Heritage Cities Programme, providing the most authoritative spatial delineation available for this site.

For Mexico City, the analysis focuses solely on the Mexico City Historic Centre component (WHS 412-001) of the jointly inscribed WHS 412, excluding Xochimilco (WHS 412-002). The official UNESCO nomination boundary map for the Historic Centre (Appendix A) was georeferenced in QGIS using a Polynomial 1 transformation, with ground control points taken directly from the grid printed on the dossier maps. The core and buffer zone boundaries were then digitized by tracing the georeferenced map's linework.

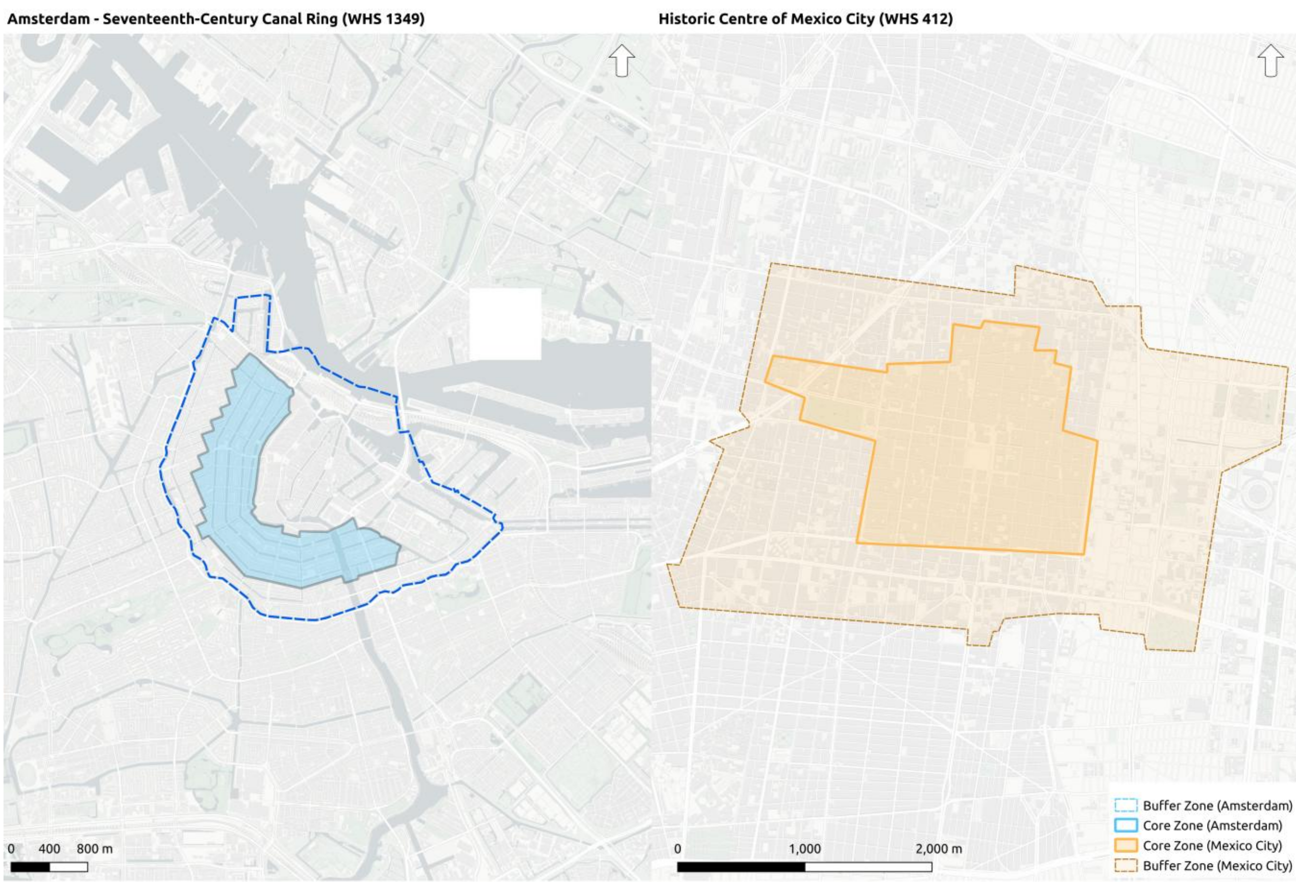

Figure 6: *Case study cities UNESCO WH boundaries*

Both Mexico City and Amsterdam case study zones are derived from official heritage boundary sources rather than arbitrary distance thresholds, ensuring a methodologically robust basis for comparative heritage risk analysis.

3.5 Spatial Data Sources

3.5.1 Tier 1: Global Datasets

The following global raster datasets were assembled and applied consistently across both case study sites, forming the basis of the Tier 1 comparative analysis.

Raster Dataset	Source	Resolution	Water Risk Type
JRC Flood Hazard (100yr)	JRC / Baugh et al., 2024	~90m	Fluvial flood depth modelling
GMIS Imperviousness	CIESIN/NASA SEDAC, 2010	30m	Pluvial flood amplification
JRC Surface Water Occurrence	JRC, 2021	30m	Permanent surface water exposure
JRC Surface Water Seasonality	JRC, 2021	30m	Seasonal water fluctuation

Table 1*: Tier 1 global spatial datasets applied across both case study sites*

3.5.2 Tier 2: Amsterdam Local Datasets

Local spatial datasets for Amsterdam were sourced from the Gemeente Amsterdam open geodata portal (maps.amsterdam.nl/open_geodata) and the Amsterdam Data Platform (data.amsterdam.nl). These datasets are maintained by municipal agencies and provide spatially precise, attribute-rich information about heritage assets, environmental conditions, and water risk at the urban scale.

Dataset	Source	Analytical Purpose
Climate Flood Hazard (Klimaateffectatlas)	Gemeente Amsterdam, 2024	Spatial model of local flood probability under climate scenarios, (4-class classification) for pluvial and fluvial flooding analysis
EGMS L3 Ground Displacement	ESA Copernicus / EGMS, 2024	SAR-derived mean annual ground velocity (2020-2024), used to identify subsidence or uplift trends affecting urban stability
Amsterdam Rainproof Drainage	Gemeente Amsterdam / Amsterdam Rainproof, 2024	Areas where drainage measures are possible and not possible
Historic Buildings (Monumentenregister)	Gemeente Amsterdam, 2024	Official registry of listed historic buildings, used to assess exposure of cultural heritage
Notable Trees (Bomen Bijzonder)	Gemeente Amsterdam, 2024	Inventory of protected trees, used to evaluate natural heritage
OSM Natural Water	OpenStreetMap contributors	Canals, waterways, and surface water features providing hydrological context

Table 2*: Tier 2 local spatial datasets for Amsterdam*

While ground displacement is not itself a water hazard, it is included as a Tier 2 contextual indicator because the primary driver of subsidence in both study areas is water-related: groundwater extraction and seasonal groundwater fluctuation. Ground displacement data therefore provides a spatially continuous proxy for the hydrological processes operating beneath the heritage zone and their cumulative impact on the built fabric

3.5.3 Tier 2: Mexico City Local Datasets

Local spatial datasets for Mexico City were sourced from the Atlas de Riesgos CDMX open data portal (atlas.cdmx.gob.mx/datosabiertos.html), produced by the Secretaria de Gestion Integral de Riesgos y Proteccion Civil (SGIRPC) and the Instituto Politecnico Nacional (IPN). Heritage asset data was sourced from OpenStreetMap via the Overpass API, queried within the WHS 412 core boundary extent.

Dataset	Source	Analytical Purpose
Waterlogging Incidents (2016-2018)	SGIRPC / Atlas CDMX	Point locations of reported waterlogging events over a 3-year period
Subsidence Zones 2016	IPN / Atlas CDMX, 2016	Broad subsidence intensity zones (2-class classification) used to identify areas with significant ground deformation
Subsidence Zones 2018	IPN / Atlas CDMX, 2018	Detailed subsidence intensity zones (5-class classification) showing spatial variation in ground deformation severity
Surface Water Bodies	SGIRPC / Atlas CDMX	Rivers, canals, and surface water features

		relevant for hydrological context
OSM Historic Buildings / Monuments	OpenStreetMap contributors	Heritage assets (points and polygons) used to assess exposure of cultural heritage

***Table 3**: Tier 2 local spatial datasets for Mexico City*

3.6 Analytical Methods

Geographic Information Systems provide a structured environment for integrating spatially heterogeneous datasets within a common coordinate framework, enabling the simultaneous analysis of multiple risk dimensions across defined spatial extents. In the context of World Heritage risk assessment, a GIS-based workflow serves a specific analytical purpose: to translate abstract risk indicators into spatially explicit outputs that can be interpreted relative to the precise boundaries of inscribed heritage properties, their designated buffer zones, and the urban fabric within which they are embedded. This spatial analysis is essential because water-related events threating WH do not operate uniformly across a city but manifest at specific locations determined by geology, hydrology, urban morphology, and infrastructure condition. A GIS workflow makes these spatial patterns visible, measurable, and comparable across sites.

The analytical workflow developed for this research was designed around three core requirements. First, it needed to be reproducible: all operations were executed using open-source software (QGIS 3.22) and openly available datasets, ensuring that the analysis can be verified, extended, or replicated by other researchers without proprietary tools or data access constraints. Second, it needed to be scalable: the tiered structure separates globally consistent datasets applicable to any World Heritage Site from locally specific datasets that depend on city-level data availability, allowing the framework to be applied where rich local data exists and in partial form where it does not. Third, the workflow was designed to produce outputs that distinguish between what the data directly shows and what it implies, acknowledging the resolution, temporal, and methodological limitations of each input dataset. The specific methods employed within this workflow are described in the following subsections.

3.6.1 Tier 1: Zonal Statistics

Zonal statistics were computed on both the core and buffer WH boundary zones on both case study cities using the QGIS native:zonalstatisticsfb algorithm, executed via a custom Python batch script within the QGIS 3.22 Python console. The method extracts and summarises the pixel values of a raster dataset that fall within the spatial extent of a vector polygon, producing quantitative descriptors of threat exposure for each defined zone. This approach is widely used in spatial risk assessment and is consistent with methodological frameworks employed in comparable heritage flood risk studies (Arrighi, 2021; Ginzarly et al., 2024).

Four statistical metrics were computed for each raster-polygon combination, each serving a distinct analytical purpose. The **mean** represents the average pixel value across all pixels within the zone, providing an overall indicator of exposure intensity that accounts for the full spatial distribution of values. The **minimum** and **maximum** values define the range of conditions present within the zone, identifying both the least and most severely exposed locations within each boundary. The **majority** represents the most frequently occurring pixel value, equivalent to the statistical mode, and indicates the dominant condition across the zone without being influenced by outliers or extreme values. For datasets where a large proportion of pixels carry zero or no-data values, such as the JRC Surface Water Occurrence layer in urban contexts, the majority is a more robust indicator of prevailing conditions than the mean.

The distinction between mean and majority is particularly relevant in this research context. In both heritage zones, urban pixels with zero surface water occurrence or zero imperviousness are numerous, tending to pull the mean toward lower values. The majority value cuts through this distributional noise to identify the most prevalent condition, which is analytically more meaningful for characterising the dominant risk exposure of a heritage zone. Both metrics are reported in Table 4 and interpreted together throughout the results chapters.

Statistics were computed using QGIS 3.22 statistic codes: Mean (2), Minimum (5), Maximum (6), and Majority (9). Analysis was conducted across four spatial zones: the Amsterdam core zone, the Amsterdam buffer zone, and the Mexico City Historic Centre core zone, and its outer buffer zone. All outputs were saved as GeoPackage files and loaded into the QGIS project for attribute inspection and verification. The analytical workflow is illustrated conceptually in Figure 7.

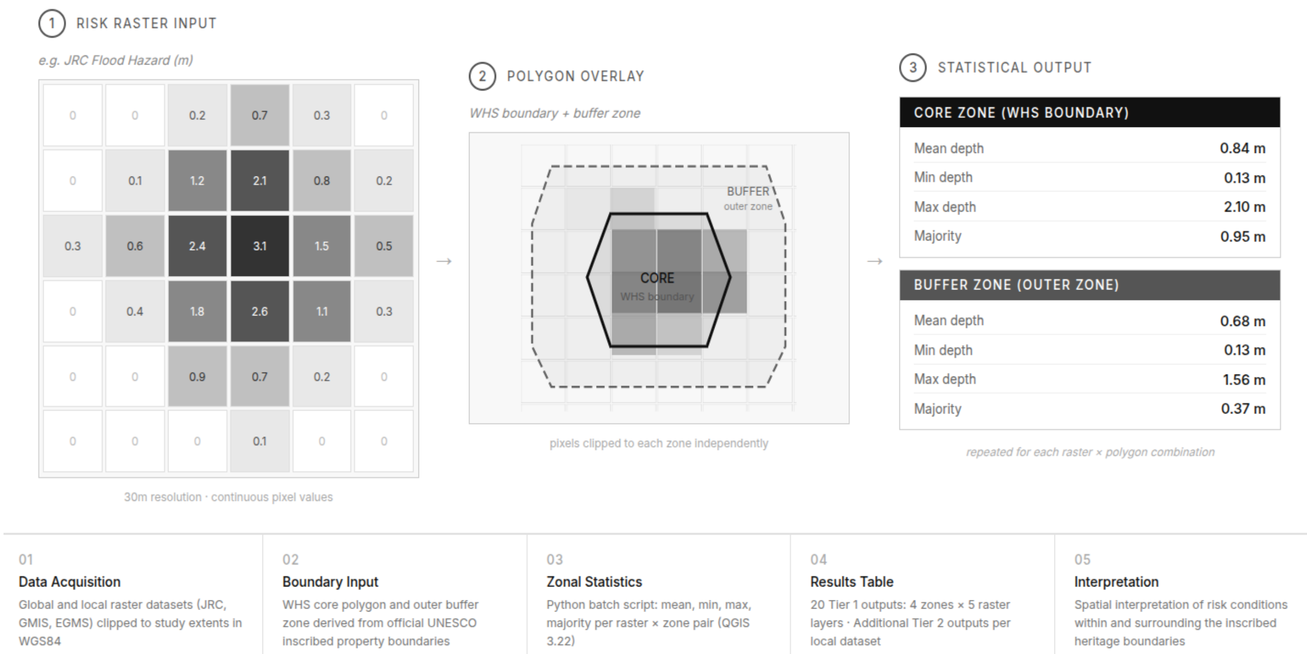

***Figure** 7: Conceptual diagram illustrating the zonal statistics workflow applied across Tier 1 global, and Tier 2 local Amsterdam analyses. Risk raster pixel values are extracted and summarized independently for each spatial zone (WHS core boundary and outer buffer zone), producing mean, minimum, maximum, and majority geo-statistics per raster-zone combination. The process was applied across five global raster datasets for four spatial zones, generating 20 Tier 1 analytical outputs, and was additionally applied to a local dataset of EGMS ground motion for Amsterdam. Statistical values shown are illustrative, based on the order of magnitude of flood depth values recorded in the Mexico City buffer zone (JRC, 2024). Actual results are presented in Tables 4 and 5. Darker shading in the raster grid corresponds to higher values.*

3.6.2 Core and Buffer Boundary Analysis

The selection of spatially distinct, heritage-defined boundary zones forms the foundation of the comparative analytical framework. Rather than applying arbitrary distance buffers, this research employs official inscribed property boundaries and their designated outer zones as the two analytical units for each city. This decision is methodologically significant: the inscribed boundary represents the area of primary OUV, while the outer zone is a ring that excludes the core and captures the designated heritage buffer immediately surrounding the inscribed property. Computing zonal statistics independently across both zones for each risk layer generates a matrix of indicator values: four zones across five raster datasets, producing twenty spatial metrics in total. The permutation of these metrics across zones enables structured comparison of how risk conditions inside the inscribed boundary relate to those in the immediately adjacent heritage setting, revealing whether risk is spatially concentrated within the OUV boundary or extends outward into the surrounding transition zone. This produces both quantitative outputs for direct comparison and a qualitative spatial narrative about the relationship between water risk and the defined heritage extent. Non-overlapping zone geometries ensure that each pixel contributes to only one zone per computation, preserving the statistical independence necessary for valid cross-zone comparison.

3.6.3 Spatial Overlay and Map Composition

Spatial overlay analysis was conducted through visual inspection and layer stacking within QGIS, with raster layers assigned distinct colour ramps to enable simultaneous interpretation of multiple risk indicators. Five thematic map compositions (Figures 8 to 11) were produced for the Tier 1 global analysis. Two additional risk maps (Figures 13a and 13b) were produced using city-specific local datasets to support the Tier 2 contextual analysis. All figures were exported as PNG images at 300 dpi for thesis integration.

3.7 Limitations and Data Comparability

Several methodological limitations are acknowledged. The GMIS imperviousness dataset is dated to 2010, predating the 2020-2025 study period. It is used as a baseline structural indicator of urban fabric density, consistent with its application in comparable heritage risk assessments (Katontoka et al., 2024), and its temporal limitation is noted as a caveat in the interpretation of imperviousness findings.

The JRC 100-year flood hazard raster excludes areas protected by engineered flood defences exceeding the 100-year return period threshold. For Amsterdam, this results in no-data values across the WHS zone, which is treated as an analytical finding reflecting the effectiveness of the city's water management infrastructure rather than a data error. This interpretation is supported by Amsterdam's Climate Flood Hazard (Klimaateffectatlas) dataset which likewise shows no significant flood probability within the canal ring core zone.

Heritage building data for Mexico City was sourced from OpenStreetMap via the Overpass API, reflecting community-contributed geographic data of variable completeness. This contrasts with Amsterdam's municipally maintained Historic Buildings (Monumentenregister) dataset, which provides consistent attribute completeness and spatial accuracy. This asymmetry is noted as a limitation of the local-scale heritage exposure comparison and reflects broader disparities in open heritage GIS data availability between European and Latin American contexts, consistent with the geographic reporting bias identified in Li (2024).

4. RESULTS: TIER 1 GLOBAL COMPARATIVE ANALYSIS

4.1 Introduction

This chapter presents the results of the Tier 1 global comparative analysis, employing standardised, globally consistent datasets to assess water-related risks at the Amsterdam Canal Ring (WHS 1349) and the Historic Centre of Mexico City (WHS 412-001) between 2020 and 2025. Note that WHS 412 is jointly inscribed with Xochimilco (412-002); however, this analysis focuses exclusively on the Historic Centre component. The analysis addresses Research Questions 1, 2, 3, and 4 by evaluating flood hazard exposure, surface water dynamics, urban imperviousness, and the implications of these indicators for OUV. Results are reported as zonal statistics across four spatial zones: the Amsterdam core, the Amsterdam buffer zone, and the Historic Centre of Mexico City core and buffer zone. Zonal statistics are summarised in Table 4.

4.2 Flood Hazard Assessment

4.2.1 Global Flood Hazard: JRC 100-Year Return Period

The JRC Global River Flood Hazard raster, modelling water depth in metres under a 100-year return period event, was overlaid with heritage boundary polygons for both case study sites to assess modelled flood exposure (Figure 8). This dataset provides a globally standardised baseline for flood risk comparison and is one of the primary data sources cited in the literature review as a basis for global-scale heritage flood risk assessment (Arrighi, 2021).

4.2.2 Amsterdam: Absence of Modelled Flood Hazard

The JRC flood hazard raster returns no-data values across all Amsterdam zones. Both the core and the buffer area return no modelled flood depth data. This finding is consistent with the JRC model's exclusion of areas protected by engineered flood defence systems exceeding the 100-year return period threshold. The Netherlands' integrated water management infrastructure, including the national dike network, polder systems, and Amsterdam's municipal pumping and canal regulation systems, effectively removes the WHS zone from the globally modelled flood hazard classification. The UNESCO description of the Amsterdam Canal District highlights the historical development of these dike and polder systems as foundational to the city's urban form and hydrological control (UNESCO World Heritage Centre, 1987)). The JRC global river flood hazard model does not account for man-made flood protection infrastructure such as dikes and levees that may already be in place in populated regions (Baugh et al., 2024; CLIMAAX, 2024). This result is not interpreted as a data absence but as an analytically significant finding: Amsterdam's heritage core exists within a zone of engineered hydrological protection that renders conventional global flood hazard modelling inapplicable at this scale.

4.2.3 Mexico City: Active Flood Exposure in the Buffer Zone

The Mexico City Historic Centre core boundary (UNESCO 412-001) returns no modelled flood data under the JRC 100-year return period scenario. The outer zone surrounding the inscribed boundary, however, records active flood exposure with a mean depth of 0.68 metres, a minimum of 0.13 metres, and a maximum of 3.70 metres. The majority value of 0.37 metres confirms that moderate flood depths are the most spatially prevalent condition across the outer buffer zone. This is a significant finding for heritage management: the buffer zone of WHS 412-001 is directly exposed to modelled flood events under a 100-year return period scenario, meaning the urban fabric, infrastructure, and communities that constitute the immediate heritage setting of the inscribed property face active flood risk. The designation of a buffer zone under the World Heritage Convention is intended to protect the integrity and setting of the inscribed property, and modelled flood exposure within that zone represents a direct threat to the conditions that sustain the OUV of the Historic Centre

4.2.4 Comparative Interpretation

The contrast between the two sites reveals fundamentally different flood risk characters. Amsterdam's heritage core is characterised by the complete absence of modelled flood exposure due to engineered protection, while Mexico City's historic zone faces active, spatially pervasive flood risk in its surrounding urban fabric. This divergence reflects not only differences in hydrological geography but also the differential investment in and effectiveness of water management infrastructure between the two contexts. Importantly, the absence of modelled flood hazard in Amsterdam does not indicate absence of water risk. Rather, it redirects analytical attention toward alternative water risk mechanisms, which are explored in Chapter 5.

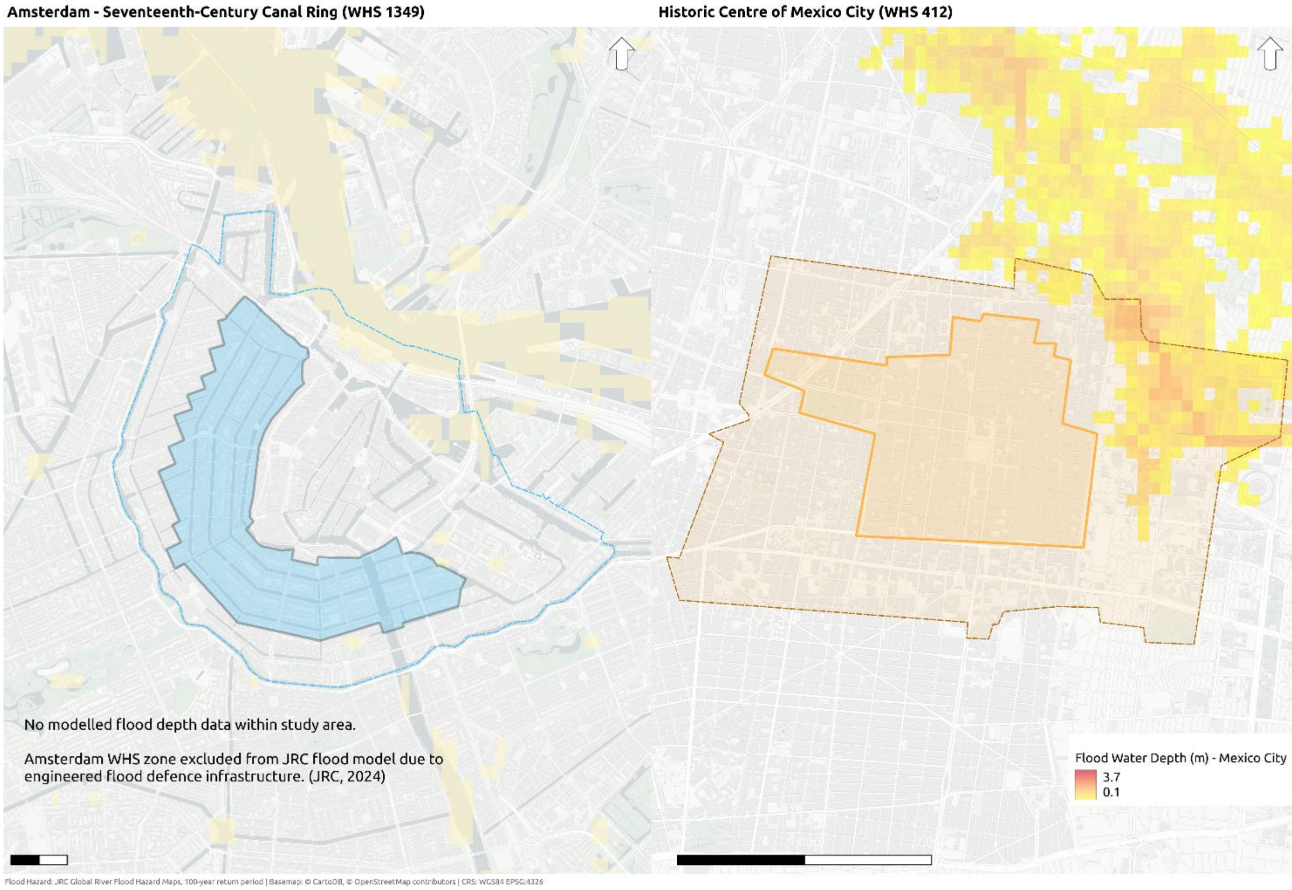

***Figure 8**: Flood Hazard Assessment, Amsterdam Canal Ring (WHS 1349) and Historic Centre of Mexico City (WHS 412-001)*

4.3 Urban Imperviousness

4.3.1 Global Imperviousness Distribution

The Global Man-made Impervious Surface (GMIS) dataset, derived from Landsat imagery, was used to assess urban surface sealing across both heritage zones (Figure 9). Pixel values range from 0 to 255, representing a linear scale from 0% to 100% imperviousness. Values were interpreted on this scale without rescaling, with zero-value pixels rendered as transparent to distinguish water bodies and vegetation from sealed urban surfaces.

4.3.2 Amsterdam: Canal Network Moderates Zonal Imperviousness

The Amsterdam Canal Ring core zone exhibits a mean imperviousness of 70.9 out of 255 (27.8%) with a majority value of 100 (39.2%). The lower mean relative to the majority reflects the significant proportion of open water pixels within the boundary, as the canal network constitutes a non-impervious fraction of the total heritage area that reduces the zone-wide average while the urban fabric between canals remains densely sealed. The outer heritage buffer zone shows a mean of 81.7 (32.0%) with a majority of 100, indicating that the broader zone is more uniformly sealed than the canal-rich core.

4.3.3 Mexico City: Uniformly Sealed Historic Core

The Mexico City Historic Centre core zone exhibits a mean imperviousness of 90.2 out of 255 (35.4%) with a majority value of 100 (39.2%), higher than Amsterdam across mean metrics. The outer buffer zone shows a similarly high mean of 85.8 (33.6%) with a majority of 100. This pattern reflects the more uniformly sealed character of the Mexico City historic centre, where the absence of an internal waterway network signifies that impervious surface dominates throughout the boundary.

4.3.4 Implications for Pluvial Flood Risk

Although Mexico City exhibits higher mean imperviousness (35.4%) than Amsterdam (27.8%) at the core zone level, the risk implications of surface sealing differ substantially between the two sites due to their contrasting drainage contexts. Amsterdam's lower mean imperviousness is partly a function of the canal network reducing the zone-wide average, and those same canals provide an integrated surface drainage pathway that discharges rainfall runoff directly. Mexico City's historic centre, by contrast, sits within a closed hydrological basin with no natural outlet, and its drainage infrastructure is compromised by differential land subsidence. Runoff that cannot infiltrate the impermeable lacustrine clay has nowhere to discharge, accumulating at the surface and generating the recurring waterlogging incidents documented in the SPC_Encharcamientos data (Chapter 5). Imperviousness therefore amplifies pluvial flood risk more severely in the Mexico City context, not because sealing is uniformly higher, but because the absence of discharge pathways means that even moderate rainfall generates surface accumulation.

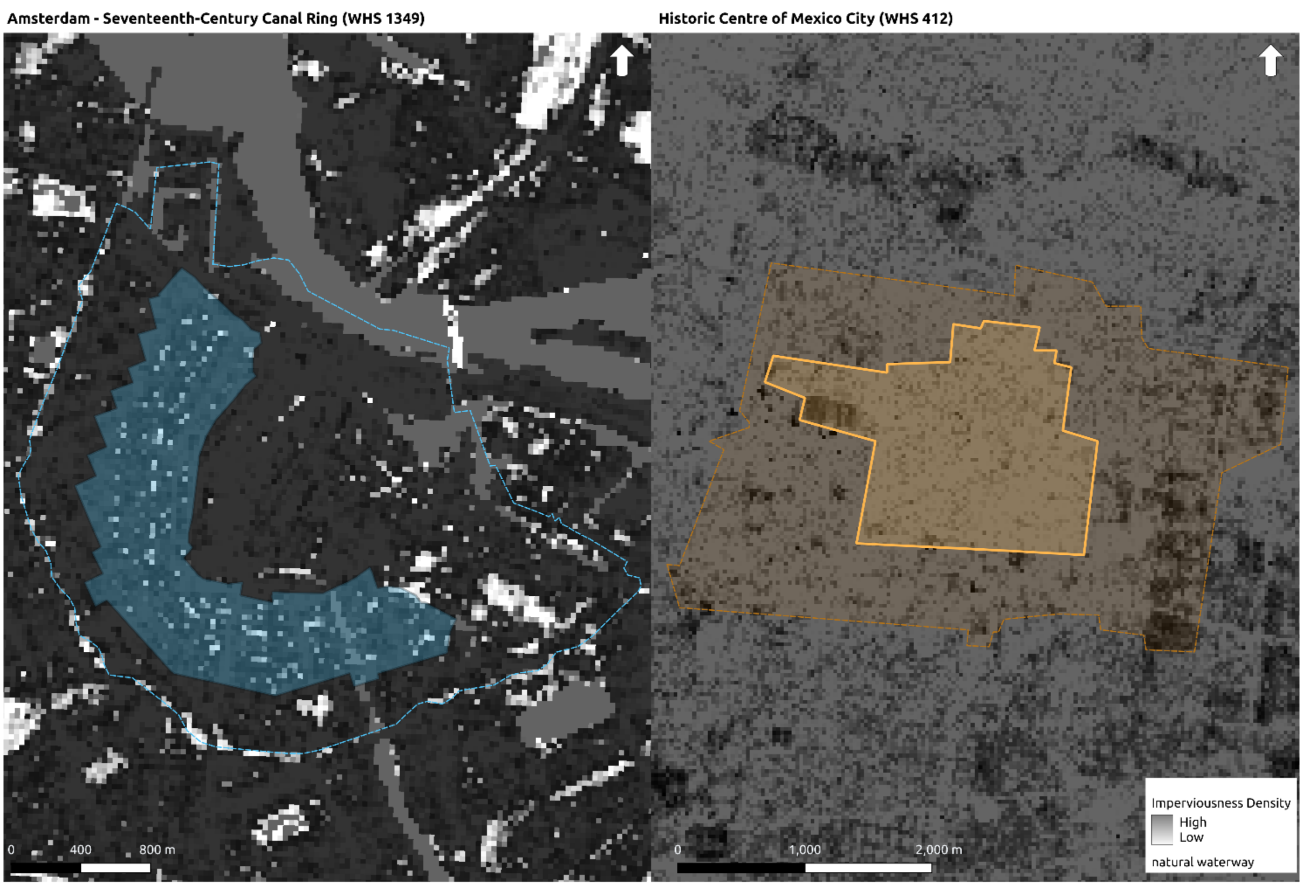

Figure 9: Imperviousness Assessment, Amsterdam Canal Ring (WHS 1349) and Historic Centre of Mexico City (WHS 412-001)

4.4 Surface Water Occurrence

4.4.1 Permanent Water Presence

The JRC Global Surface Water Occurrence dataset, recording the percentage of time a pixel was classified as water between 1984 and 2021, was overlaid with heritage boundaries to characterise the permanent and episodic water presence at both sites (Figure 10). Pixels with occurrence values of zero were rendered as transparent, ensuring that only meaningful water detection is visualised. To accompany the surface water raster signal, the physical waterway network of each city, surface water and drainage channel vectors are overlaid on both study areas. For Amsterdam, the OSM canal vectors confirm spatial correspondence with the high-occurrence pixels, though the 30m JRC resolution captures only the wider principal canals. The narrower, secondary channels of the canal ring fall below the detection threshold and are better represented by the vector layer. For Mexico City, the surface drainage channel layer (Atlas de Riesgos CDMX) documents the drainage courses traversing mostly within the buffer zone of WHS 412-001. The near-zero surface water occurrence values recorded across the Mexico City zones are consistent with the engineered drainage of the former Lake Texcoco lakebed.

4.4.2 Amsterdam: Persistent Canal Network

The Amsterdam core zone exhibits a mean surface water occurrence of 1.40%, reflecting the spatially limited but extremely high-occurrence canal pixels within the dense urban fabric. The maximum occurrence value of 97% confirms near-permanent water presence within the core, corresponding to the historic canal network that defines the site's OUV.

The outer heritage zone shows a higher mean of 6.58% and a maximum of 99%, reflecting the greater proportion of waterway surface relative to urban fabric in the broader buffer area. The majority value of 0 across both Amsterdam zones confirms that surface water pixels are spatially concentrated rather than distributed, with the canals occupying a small but permanent fraction of the total heritage area.

4.4.3 Mexico City: Hydrological Sealing of Former Lakebed

The Mexico City core zone returns an absolute mean surface water occurrence of 0%, with minimum, maximum, and majority all equal to zero. This result confirms that no surface water was detected at any point within the precise Historic Centre boundary during the entire 37-year observation period, reflecting the near-complete drainage and urbanisation of the former Lake Texcoco lakebed. The outer buffer zone shows a marginally higher mean of approximately 0.002% and a maximum of 25%, indicating the presence of some episodic surface water at the periphery of the boundary. The contrast with Amsterdam could not be more complete: where Amsterdam's heritage is defined by living surface water, Mexico City's is defined by its complete absence.

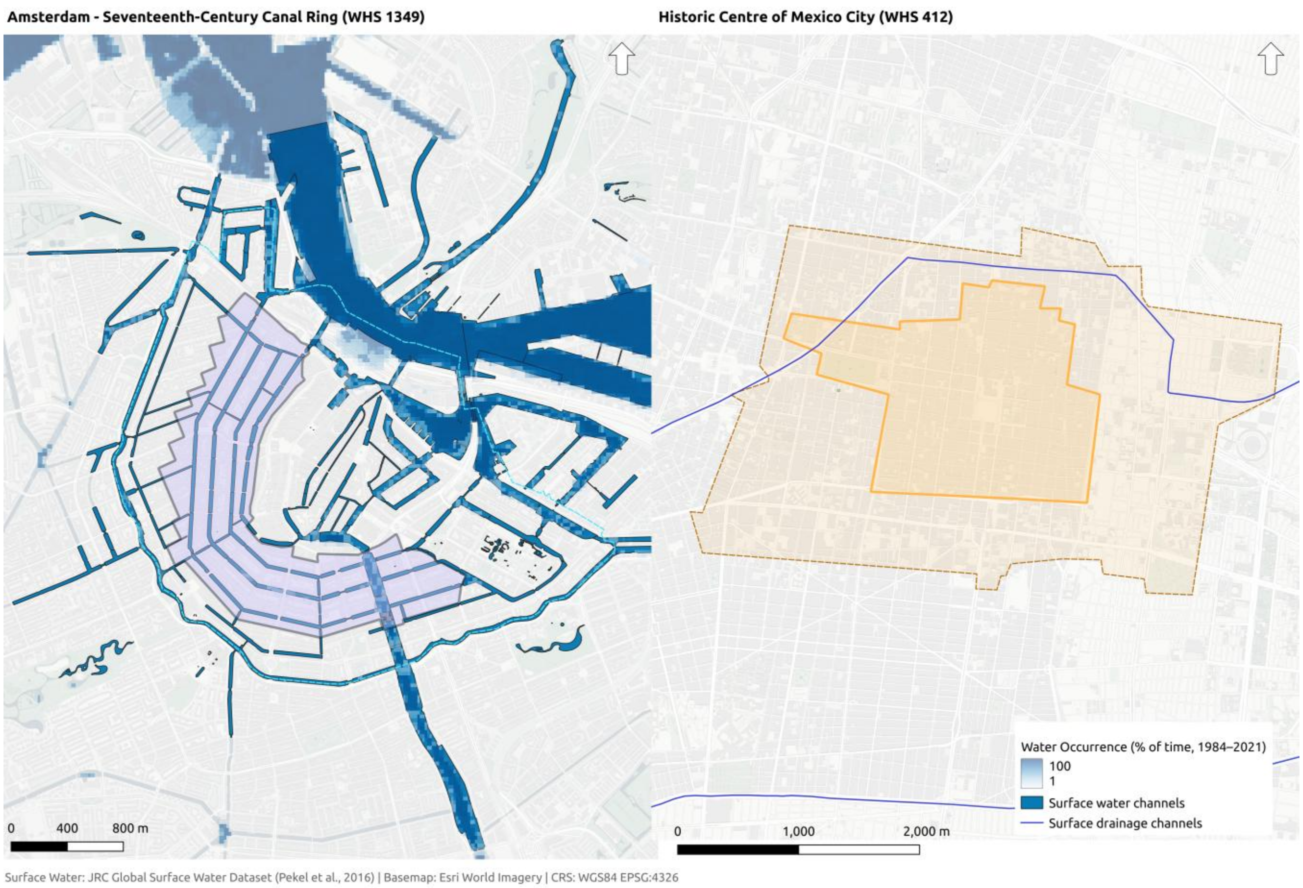

***Figure 10**: Surface Water, Amsterdam Canal Ring (WHS 1349) and Historic Centre of Mexico City (WHS 412-001)*

4.5 Surface Water Seasonality

The JRC Surface Water Seasonality dataset, recording the number of months per year that a pixel was classified as water, was analysed across both heritage zones to distinguish permanent from seasonal water presence (Figure 11). Amsterdam's core zone exhibits a mean seasonality of 0.22 months and the outer heritage zone a mean of 1.00 months, with maximum values of 12 months in both zones confirming the presence of year-round permanent water bodies, primarily the canal network and surrounding waterways. Mexico City's core zone returns a mean seasonality of 0 months and the buffer zone a mean approaching 0, with maximum values of 0 and 8 months respectively. The near-zero mean values confirm that seasonal water presence is not a dominant characteristic of the Historic Centre zone, consistent with the absence of surface water occurrence findings.

Together, the surface water occurrence and seasonality findings reinforce a fundamental distinction in the hydrological character of the two sites: Amsterdam's water risk is associated with living, permanent surface water that forms the physical basis of the site's OUV, while Mexico City's water risk is driven by the consequences of water removal, including subsidence, drainage failure, and the hydrological instability of the former lakebed, rather than by surface water presence itself.

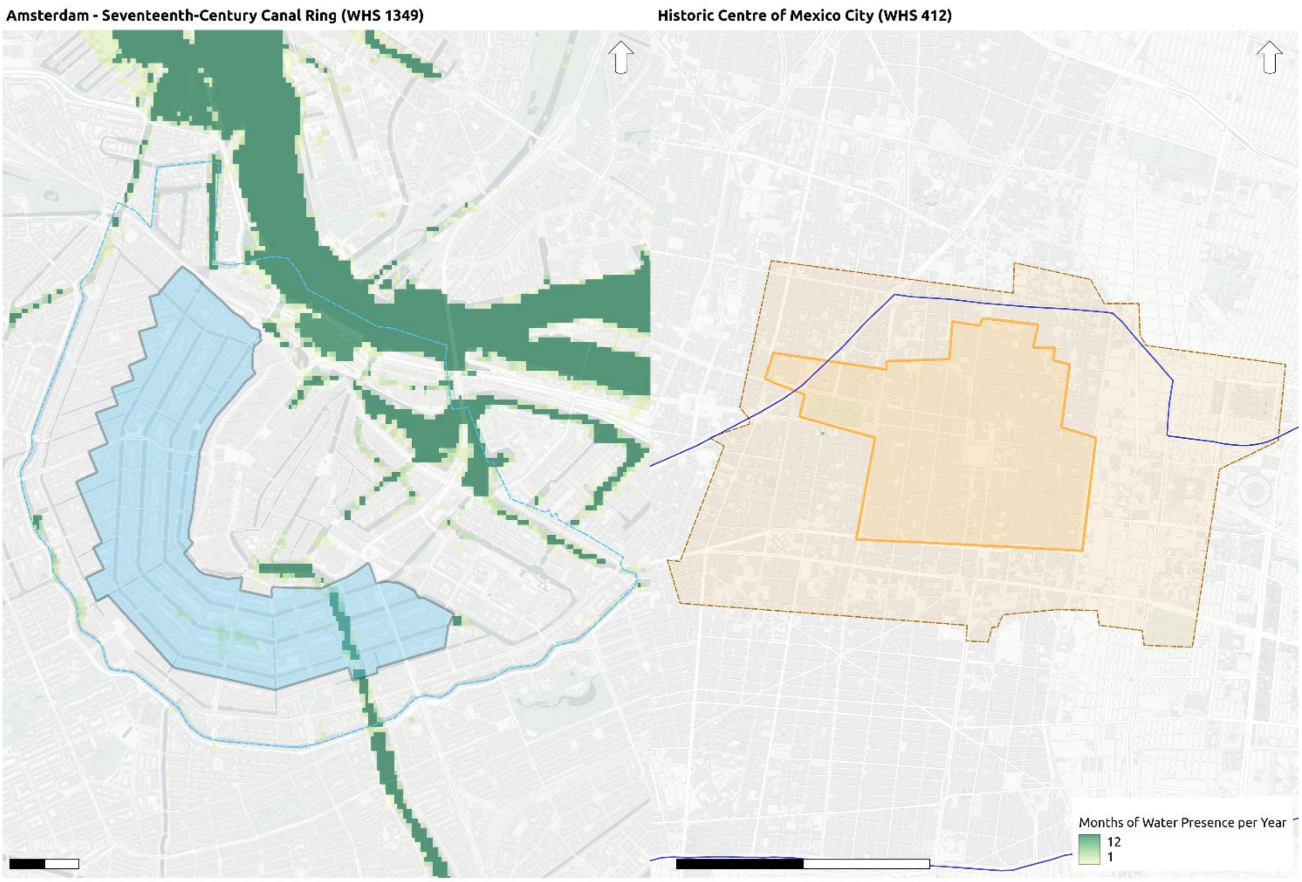

Figure 11*: Surface Water Seasonality, Amsterdam Canal Ring (WHS 1349) and Historic Centre of Mexico City (WHS 412-001)*

4.6 Change Intensity

The JRC Surface Water Change Intensity dataset was analysed to assess hydrological change within both heritage zones. Majority values of 253 were recorded across all four analytical zones for both cities. In the JRC encoding, a value of 253 indicates that the dominant land cover class was never classified as surface water at any point during the 1984-2021 observation period. This result is consistent with the urban character of both heritage zones and confirms that neither site is experiencing a surface water expansion or contraction process detectable from satellite observation. This finding further reinforces the argument that water risk at both WH sites are driven by subsurface and pluvial mechanisms rather than surface hydrological change.

4.7 Zonal Statistics Summary

Table 4 presents the complete zonal statistics results for all Tier 1 global datasets across all four analytical zones, reporting mean values per zone.

Layer / Metric	AMS Core	AMS Buffer	MEX Core	MEX Buffer
Flood depth (m)	No data	No data	No data	0.68m
Imperviousness (%)	27.8%	32.0%	35.4%	33.6%
SW Occurrence (%)	1.40%	6.58%	0%	~0%
Seasonality (months)	0.22	1.00	0	~0
Change intensity	249.2	239.7	253.0	253.0

***Table 4**: Tier 1 global zonal statistics: mean values per zone. Flood: Amsterdam WHS zone excluded from JRC model (engineered defence); AMS buffer returns uniform code value of 1.0 (not a depth in metres). MEX core returns no data; flood exposure confirmed in buffer only (max 3.70m, majority 0.37m). Imperviousness converted from 0-255 GMIS scale to percentage. Change intensity majority 253 = never-water; urban fabric across all zones.*

4.8 Tier 1 Summary: Comparative Findings

The Tier 1 global comparative analysis reveals five principal findings that characterise the divergent water risk profiles of the two case study sites.

- First, flood hazard is absent from the Amsterdam heritage zone under the JRC global model, and active in the surrounding zone of Mexico City's historic centre, reflecting fundamentally different flood risk characters: engineered protection on one hand, and active exposure on the other.

- Second, Mexico City's historic centre exhibits higher mean imperviousness (35.4%) than Amsterdam's canal ring core (27.8%), though Amsterdam's majority value indicates equivalent dense sealing between canal channels. The canal network offsets impervious sealing effects by providing discharge pathways, while Mexico City's closed basin and subsidence-damaged drainage mean equivalent sealing produces greater flood accumulation.

- Third, permanent surface water is spatially concentrated within Amsterdam's heritage zone through the canal network (maximum occurrence 97%) and entirely absent from Mexico City's core zone (maximum occurrence 0%), representing the most complete contrast between the two sites.

- Fourth, seasonal water presence at Amsterdam is confirmed by the buffer zone mean seasonality of 1.00 months, while Mexico City shows no meaningful seasonal water signal within either zone, consistent with the complete hydrological sealing of the former lakebed.

- Fifth, both sites show uniform change intensity majority values of 253 across all zones, confirming that neither faces surface hydrological expansion but that both face water risks operating through subsurface and pluvial mechanisms invisible to satellite surface water detection.

5. RESULTS: TIER 2 LOCAL CONTEXTUAL ANALYSIS

5.1 Introduction: Rationale for Local Analysis

The Tier 1 global analysis established the comparative water risk profiles of Amsterdam and Mexico City at the macro scale. However, the global datasets employed in that analysis are unable to capture the site-specific heritage vulnerabilities, local hydrological dynamics, and urban fabric characteristics that determine how water risk translates into actual damage to OUV. This chapter presents the Tier 2 local contextual analysis, drawing on city-specific datasets sourced from national and municipal agencies to provide more granular insight into the water risk exposure of each heritage site.

The local datasets assembled for Amsterdam and Mexico City are not directly comparable in methodological terms, reflecting the inherent asymmetry between the mature open GIS infrastructure of Dutch municipal governance and the more heterogeneous data landscape of Mexican risk management agencies. This asymmetry is itself an empirical finding of this research: the contrast between Amsterdam's purpose-built, consistently maintained municipal risk datasets and Mexico City's multi-agency, multi-epoch survey products was encountered directly during data acquisition and reflects broader regional disparities in open spatial data availability for heritage risk assessment. Rather than forcing false comparability, this analysis treats each city's local dataset as a contextually appropriate evidence base for understanding the site-specific dimensions of water risk for further comparability in Chapter 6.

5.2 Amsterdam Canal Ring: Local Risk Profile

5.2.1 Geological and Hydrological Context

The Amsterdam Canal Ring WHS is situated on reclaimed bogland and peat subsoil, with ground elevations ranging from approximately −4 metres to +2 metres relative to the Amsterdam Ordnance Datum (NAP), consistent with AHN national elevation data that places much of the western Netherlands between −5 metres and +25 metres NAP (Deltares, 2014). The historic urban fabric is founded on wooden piles driven into the peat subsoil during the 17th-century construction of the canal ring.

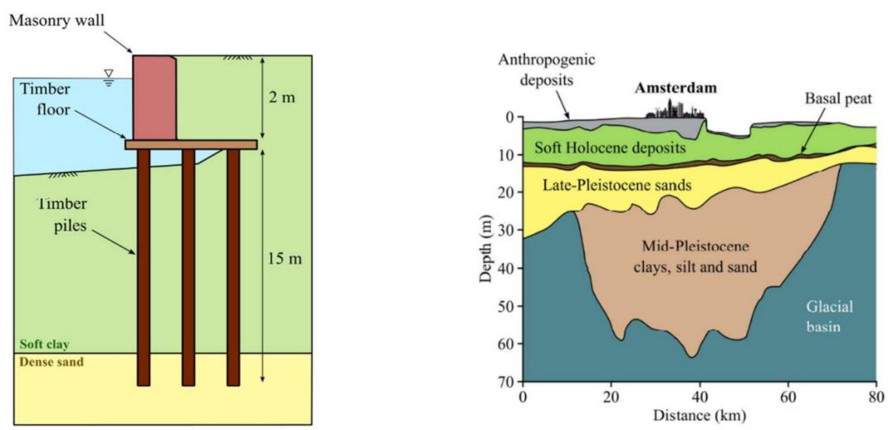

***Figure 12**: [left] Example 20th century urban quay (a), [right] geological cross-section of Amsterdam (b) (Duffy & Gavin, 2023)*

The structural integrity of these foundations is directly dependent on maintaining a stable groundwater table: the piles must remain permanently submerged, as exposure to oxygen initiate's rapid biological decay. This groundwater dependency is well documented in Dutch geotechnical research, which shows that fluctuations in groundwater levels accelerate fungal degradation and reduce the load-bearing capacity of timber pile foundations. Both excessive groundwater rise and groundwater depletion therefore constitute risk conditions for the heritage fabric.

SAR-derived ground motion data from the European Ground Motion Service (EGMS Level 3, 2020-2024) provides a spatially continuous measurement of mean annual ground velocity across the Amsterdam heritage zone, enabling direct quantification of subsidence and uplift rates within and surrounding the inscribed boundary. This dataset directly parallels the SPC-IPN subsidence survey data employed in the Mexico City Tier 2 analysis, strengthening the comparability of the local risk profiles across both case studies.

5.2.2 Infiltration Classification: Amsterdam Rainproof

The Amsterdam Rainproof programme classifies areas of the city according to their rainwater infiltration capacity, identifying zones where shallow groundwater conditions reduce or eliminate the soil's ability to absorb surface water during intense rainfall events. Two classifications are relevant to this analysis: Niet Mogelijk, indicating areas where no rainwater infiltration is possible, and Mogelijk, indicating areas where infiltration is possible with intervention. Both classifications reflect conditions where elevated groundwater tables constrain the city's natural drainage response to extreme precipitation, increasing surface vulnerability to waterlogging and pluvial flooding.

Analysis of this layer against the heritage boundary reveals that areas of limited and absent infiltration capacity are spatially present within and immediately adjacent to the canal ring heritage area. Visual inspection of the spatial coincidence between the Heritage Building layer and the infiltration classification polygons identifies one listed historic building located within a documented zone, with several additional listed structures positioned immediately adjacent to classification boundaries. While this layer does not directly measure chronic groundwater levels or their structural implications for pile foundations, the spatial presence of constrained infiltration capacity within the heritage zone is relevant to both surface flood vulnerability during extreme rainfall and the foundation integrity risk discussed below. A formal point-in-polygon intersection quantifying individual structures and their proximity to each infiltration classification is proposed in Section 7.4.

The structural implications of groundwater behaviour are particularly significant for the 17th-century canal houses, whose timber pile foundations are subject to a bidirectional risk unique to the Amsterdam heritage context. When groundwater levels rise above their managed threshold, water infiltrates through the peat subsoil into building foundations, causing basement flooding, capillary moisture rise through historic masonry, salt crystallisation damage to brick and plasterwork, and corrosion of structural fixings embedded in foundation beams (Waternet, 2024). When groundwater levels fall during drought periods, the upper portions of wooden piles are exposed to oxygen, enabling fungal and bacterial decay that progressively weakens the foundation structure, a process confirmed in peer-reviewed literature to accelerate with increasing drought frequency and duration (Klaassen et al., 2023; Waternet, 2024). The canal houses were designed to rely on a permanently stable groundwater table and were not constructed with waterproofing measures that protect against either condition.

Under climate change projections, both the frequency of extreme precipitation events and the severity of summer droughts are expected to increase, intensifying the bidirectional groundwater risk to Amsterdam's heritage foundations and making the maintenance of a precisely regulated groundwater table an increasingly critical conservation challenge

5.2.3 EGMS Findings

EGMS Level 3 vertical ground motion data (2020-2024) reveals that the Amsterdam Canal Ring WHS zone is experiencing measurable land subsidence across both analytical zones. It should be noted that ground displacement velocity is not a direct water risk indicator but is included here as a hydrologically driven contextual variable: the subsidence measured within the Amsterdam heritage zone reflects the cumulative effect of groundwater fluctuation on the compressible peat subsoil. The inscribed core boundary shows a mean velocity of -0.85 mm/year with all pixel values negative, ranging from -0.38 to -1.60 mm/year, indicating consistent but low-magnitude subsidence throughout the entire heritage area with no zones of uplift. The buffer heritage zone exhibits greater spatial variability, with a mean of -0.95 mm/year, a minimum of -3.64 mm/year, and a maximum of +0.56 mm/year, confirming localised areas of more severe subsidence at the periphery of the heritage zone alongside limited areas of marginal uplift. The majority value of -3.64 mm/year in the buffer zone indicates that the most spatially prevalent condition is at the more severe end of the observed range, suggesting concentrated ground loss in specific areas of the outer zone. These spatial spatistics are documented in Table 5.

Zone	Mean (mm/yr)	Min (mm/yr)	Max (mm/yr)	Majority (mm/yr)
AMS Core	-0.85	-1.60	-0.38	-1.60
AMS Buffer	-0.95	-3.64	+0.56	-3.64

Table 5: *EGMS L3 Ground Motion Velocity Amsterdam WHS Zones (2020-2024)*
Negative values indicate subsidence. Positive values indicate uplift.
Source: European Ground Motion Service Level 3 (EGMS L3), Copernicus Land Monitoring Service (2024).

While these rates are orders of magnitude lower than the 92-115 mm/year subsidence documented in Mexico City (Cabral-Cano et al., 2008), the consistent negative values across the Amsterdam core confirm that ground motion is an active process within the heritage zone, with direct implications for the wooden pile foundations whose structural integrity depends on stable groundwater and soil conditions.

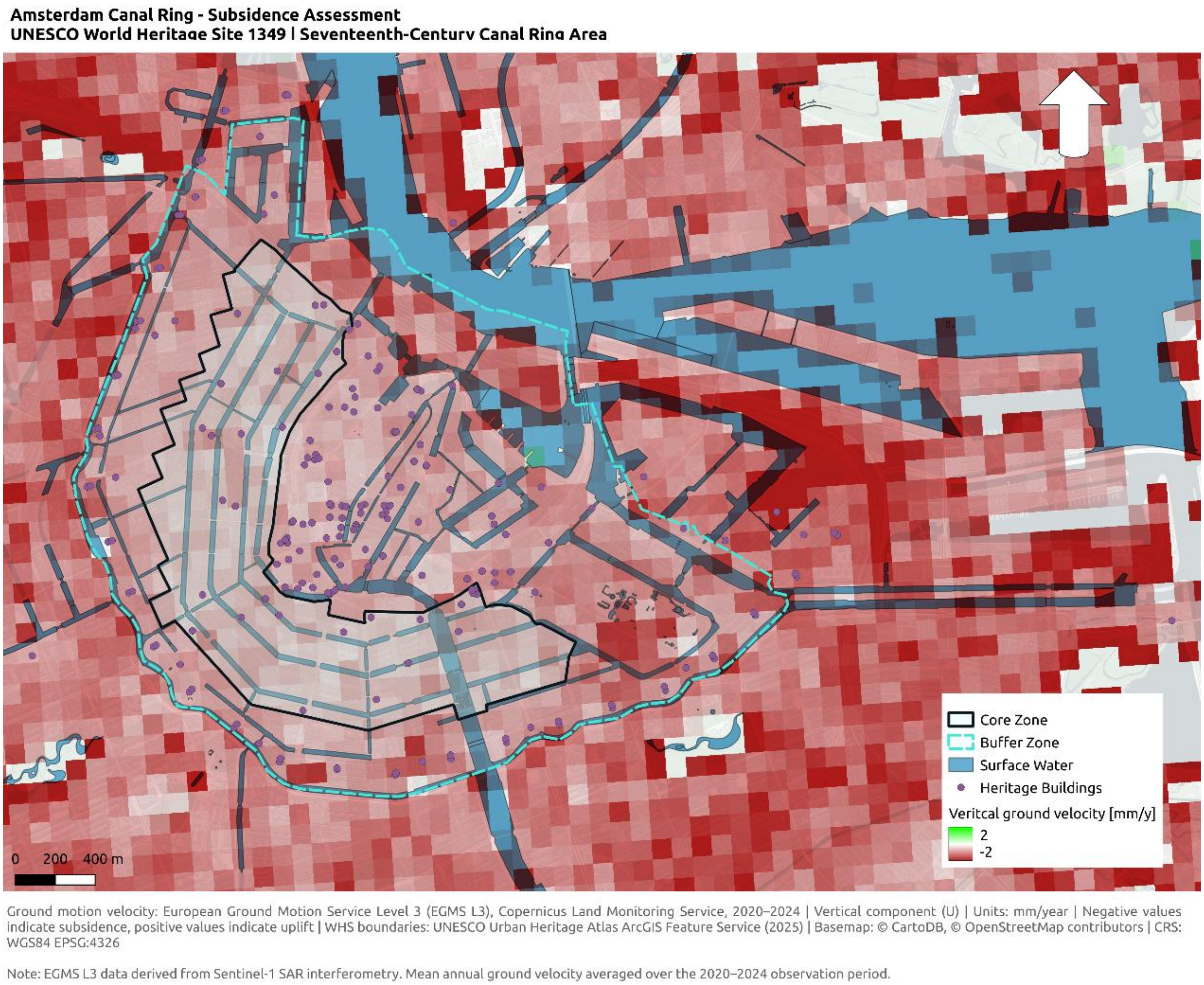

Figure 13a*: Vertical ground motion velocity (2020-2024)*

5.2.4 Local Flood Model: (Klimaateffectatlas)

The Amsterdam municipal flood probability model classifies the city's flood risk into four probability classes: no significant flood risk, extreme low probability (less than 1 in 30,000 per year), very low probability (1 in 3,000 to 1 in 30,000 per year), and low probability (1 in 300 to 1 in 3,000 per year). Spatial analysis of this layer confirms that the Amsterdam WH core zone falls within the no significant flood risk classification, consistent with the JRC global model's finding of no flood hazard within the Amsterdam heritage zone.

However, the broader buffer heritage zone and surrounding districts show variable flood probability classifications, with low and very low probability zones present north and east of the canal ring, particularly in areas adjacent to the IJ harbour. This spatial pattern confirms that the canal ring's protection is real but localised. The engineered defences create a protected envelope within which the core heritage zone sits, but residual flood risk persists at the edges of this envelope and in surrounding areas. The implication for heritage management is that the protection of the canal ring's OUV is critically dependent on the ongoing effectiveness of the infrastructure that maintains this protective envelope.

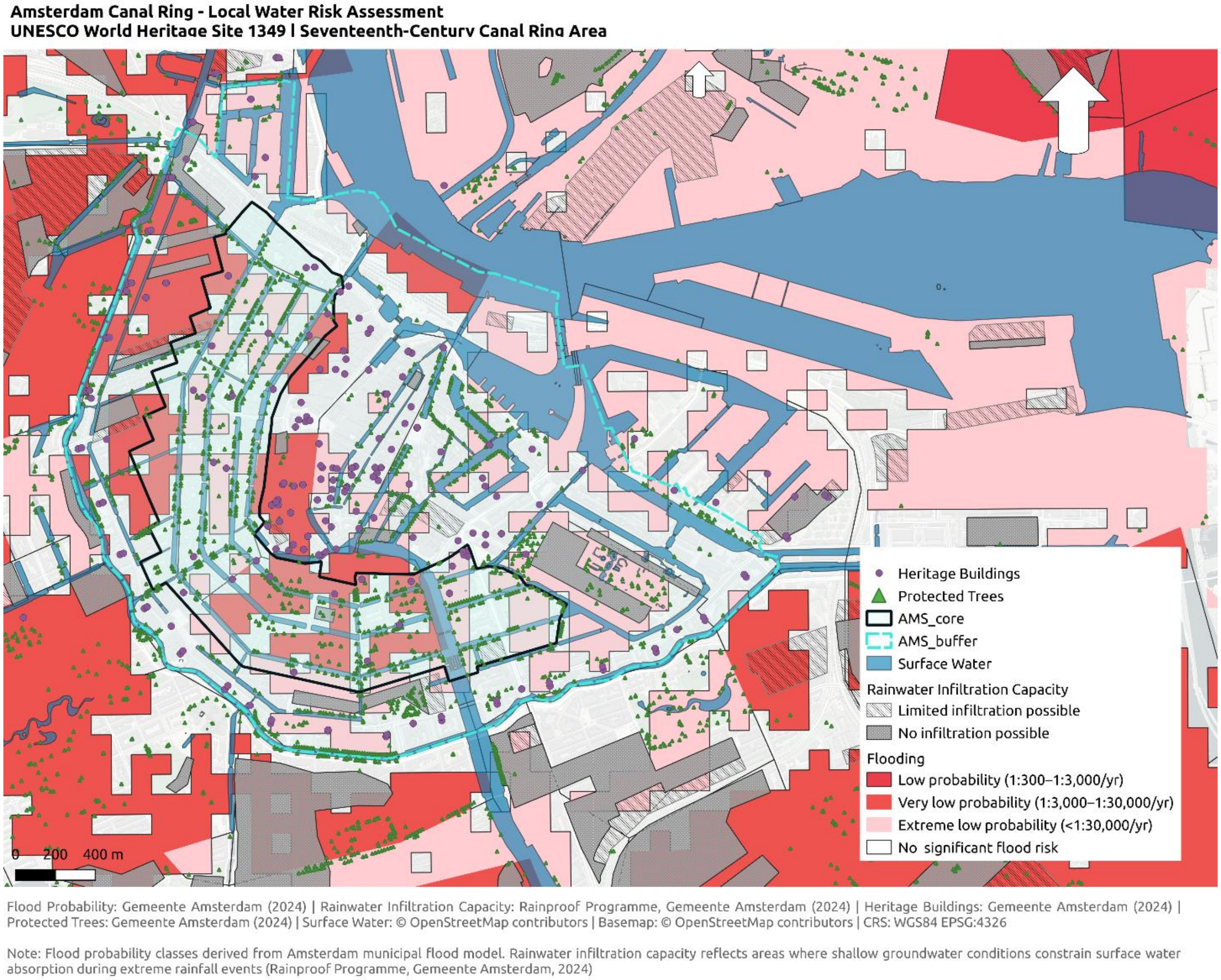

Figure 13b*: Amsterdam Canal Ring Local Water Risk Assessment.*

5.2.5 Heritage Fabric Exposure

The Heritage Buildings (Gemeente Amsterdam, 2024) layer records individually listed historic buildings as point features across Amsterdam. Visual overlay analysis with the groundwater risk, ground displacement, and flood probability layers reveals a dense concentration of listed buildings within the high groundwater risk zones, particularly within the medieval core. The Protected Trees (Gemeente Amsterdam, 2024) layer similarly shows heritage tree locations distributed across the heritage zone, with several instances of protected trees located within or adjacent to high groundwater zones. This is relevant because tree root systems and soil moisture dynamics in teract with the shallow groundwater table and the peat subsoil beneath the heritage area.

Together, these heritage asset layers confirm that Amsterdam's water risk is not an abstract spatial pattern but a direct threat to specifically identified, individually listed heritage assets. The spatial coincidence of high groundwater risk with the highest density of listed historic buildings represents the most critical intersection of hazard and heritage exposure within the site.

5.3 Historic Centre of Mexico City: Local Risk Profile

5.3.1 Geological and Hydrological Context: Former Lake Texcoco

It is important to note that Mexico City remains highly susceptible to flooding despite its elevation of approximately 2,240 metres above sea level. The Basin of Mexico is a closed lacustrine basin with no natural outlet, meaning rainfall accumulates rapidly and even small precipitation events generate immediate overland flow (Ortega, 1989). Intense summer rainfall, impermeable clay soils, extensive urbanisation, and drainage infrastructure weakened by differential subsidence all contribute to severe pluvial flooding. Following the Spanish conquest, successive drainage works progressively emptied the former lake system through canals and dikes, and by 1900 the valley had been fully drained via a 40-kilometre canal and a tunnel cut through the surrounding mountains depicted in Figure 14.

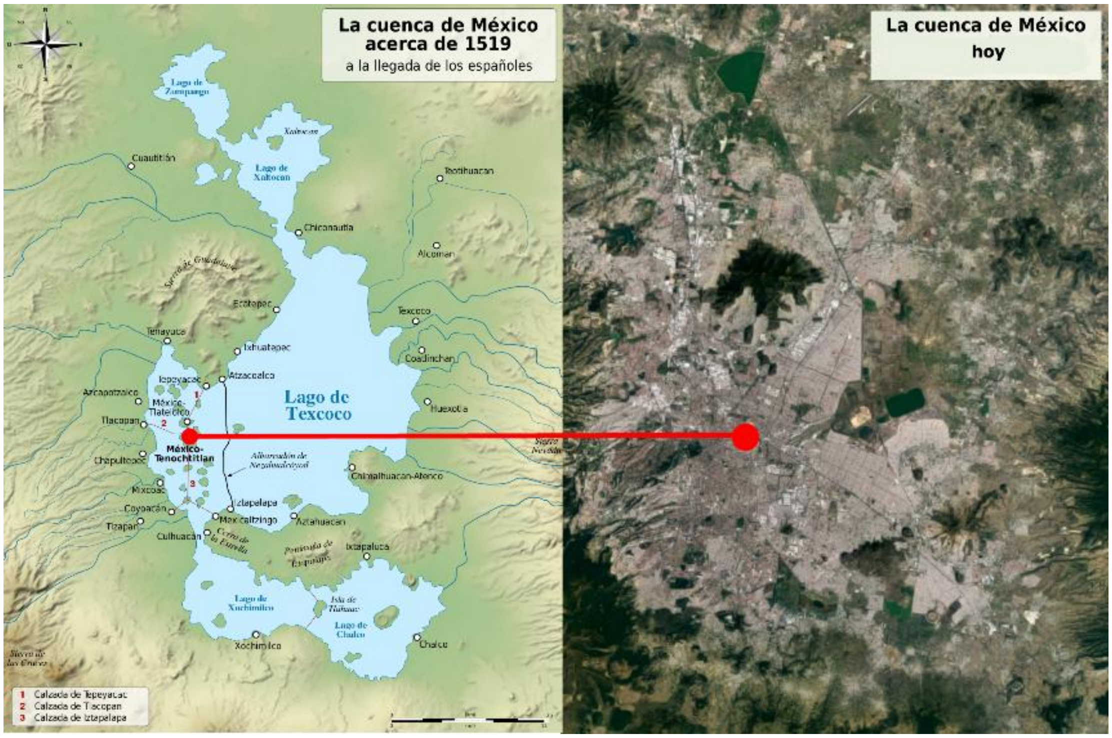

Figure 14: *The Valley of Mexico in 1519 compared with the present-day metropolitan extent, showing the near-complete drainage and urbanisation of the former lake system including Lakes Texcoco, Xochimilco, Chalco, Xaltocan, and Zumpango. The Historic Centre of Mexico City (WHS 412-001) occupies the former island of Mexico-Tenochtitlan at the centre of the former lake. Engel, J. / Decolonial Atlas (2018).*

Today, sewage and stormwater are pumped out of the basin through a large canal and tunnel system (Chaussard et al., 2021). The main parts of this system are the Gran Canal del Desagüe (Grand Drainage Canal) and the deep drainage tunnels known as the Emisor Central and Emisor Oriente. These are the modern versions of the old drainage works built after the Spanish conquest, but the basic idea is still the same: because the valley has no natural outlet, water must be pushed out of it by force. Over time, this created what researchers call a megabasin, where water is constantly brought in, moved around the city, and then pumped out again to prevent flooding (Bojorquez-Tapia et al., 2022). The problem is that land subsidence is now lowering the ground unevenly, which changes the hydraulic gradient and makes it harder for these canals and tunnels to move water efficiently. The mechanics of the changing hydrologic system is described below in Figure 15.

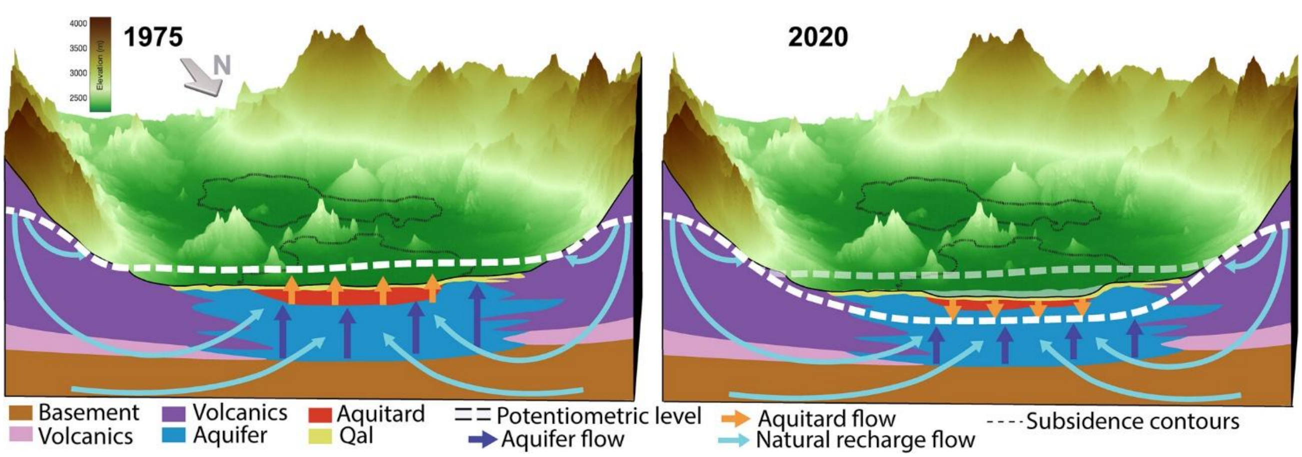

Figure 15 *Schematic representation of the water flow in the Zona Metropolitana del Valle de México (ZMVM) in 1975 (left) and in 2020 (right). (Left) Upward flow persisted across the basin floor prior to the decades of significant groundwater extraction due to recharge and infiltration from mountain runoff on the edge of the basin leading to artesian conditions. (Right) In contrast, the decades of groundwater extraction have mostly lowered the potentiometric level to a level deeper than the base of the upper aquitard, leading to downward flow of polluted water from the aquitard into the producing aquifer (Chaussard et al., 2021)*

5.3.2 Subsidence Risk: SPC-IPN Survey Data

The most consequential water-related risk to the Historic Centre of Mexico City is ground subsidence, driven by the extraction of groundwater from the underlying aquifer system. As groundwater is pumped for urban supply, the hydraulic pressure supporting the lacustrine clay layers is reduced, causing consolidation and compaction of the clay. This process manifests as measurable land surface descent. Subsidence rates in the historic centre have been documented at 92 to 115 millimetres per year using InSAR satellite data (Cabral-Cano et al., 2008), representing among the highest rates of anthropogenic land subsidence recorded in any urban heritage context globally.

Analysis of the Atlas de Riesgos CDMX subsidence survey data (SPC-IPN, 2016 and 2018) reveals that the Mexico City Historic Centre core zone falls within areas classified as having significant subsidence intensity. The 2016 survey employed a binary intensity classification (Menor and Mayor), while the 2018 survey expanded to a five-class system (Muy Bajo (Very Low), Bajo (Low), Medio (Medium), Alto (High), and Muy Alto (Very High)), reflecting methodological refinement in the intervening period. The spatial extent of the high and very high intensity classes in the 2018 survey overlaps substantially with the OSM-mapped heritage building and monument locations within and surrounding the core boundary, indicating that the most historically significant structures are also those subject to the most severe differential settlement.

Subsidence constitutes a water-induced risk because its primary driver is groundwater extraction, a human activity responding to urban water demand. The connection between urban water governance and heritage vulnerability is traceable through a clear sequence of physical processes. Municipal demand for groundwater drives extraction from the underlying aquifer system, reducing hydraulic pressure within the confined aquifer and initiating consolidation (the slow compression of water-saturated clay) of the overlying lacustrine clay deposits. As the clay compresses from reduced hydraulic pressure, the land surface descends. Since the thickness and compressibility of the lacustrine clay varies spatially across the former lakebed, the rate of descent is uneven across short distances. This *differential* subsidence imposes unequal loads on historic building foundations, threatening overall structural integrity, facade tilting, wall cracking, etc. The physical integrity of the heritage fabric and it's OUV is therefore not threatened by water arriving at the surface, but by the consequences of water being removed from beneath it, a phenomenon that could benefit from strategic, low-impact environmental engineering interventions.

5.3.3 Local Flood and Waterlogging: Encharcamientos

The Atlas de Riesgos CDMX waterlogging incident records (SPC_Encharcamientos) for 2016, 2017, and 2018 provide a three-year spatial record of reported flooding and waterlogging events across Mexico City. These point features represent locations where surface water accumulated following rainfall events, recording the practical manifestation of pluvial flood risk at street and neighbourhood level. Analysis of the three-year dataset against the Historic Centre core boundary (WHS 412-001) reveals waterlogging incidents in the vicinity of the core boundary and within the buffer zone across all three years, confirming that pluvial flooding is a recurring, multi-year phenomenon in the historic urban landscape surrounding the inscribed heritage area.

The spatial distribution of waterlogging incidents is consistent with the subsidence-induced drainage failure mechanism: as the land surface subsides differentially, drainage gradients that historically directed surface water toward outflow channels are disrupted or reversed, causing water to accumulate in low-lying areas that were previously able to drain. The spatial coincidence of high subsidence intensity zones with recurring waterlogging incident locations across the 2016-2018 Encharcamientos record suggests a compounding water risk mechanism: differential land subsidence disrupts historical drainage gradients, causing surface water to accumulate in areas that previously drained freely, thereby generating pluvial flooding as a secondary consequence of the primary groundwater extraction risk.

5.3.4 Heritage Fabric Exposure

Heritage building and monument data sourced from OpenStreetMap within the Historic Centre core boundary (WHS 412-001) confirms the presence of numerous listed historic structures, archaeological features, and cultural monuments within the zone of documented subsidence and waterlogging risk. While the completeness and attribute consistency of the OSM dataset is acknowledged as a limitation relative to the Amsterdam municipal data, the spatial density of mapped heritage features within the risk zones is sufficient to confirm that water-related risks are directly coincident with the heritage fabric rather than spatially separated from it.

The OSM heritage data provided datapoints corresponding to historic religious buildings, colonial administrative structures, and archaeological sites within the core boundary. These typologies are characterised by substantial foundation loads and masonry fabric that is particularly sensitive to the cracking and distortion caused by differential settlement. Their spatial presence within zones of documented high subsidence intensity, as mapped by the SPC-IPN surveys, indicates that the structures most significant to the OUV of WHS 412-001 are also among those most physically exposed to the dominant water-related risk mechanism at the site. This spatial correspondence, while based on visual observation rather than formal quantitative intersection, provides a preliminary indication of where heritage-specific vulnerability is greatest and where targeted structural assessment should be prioritised.

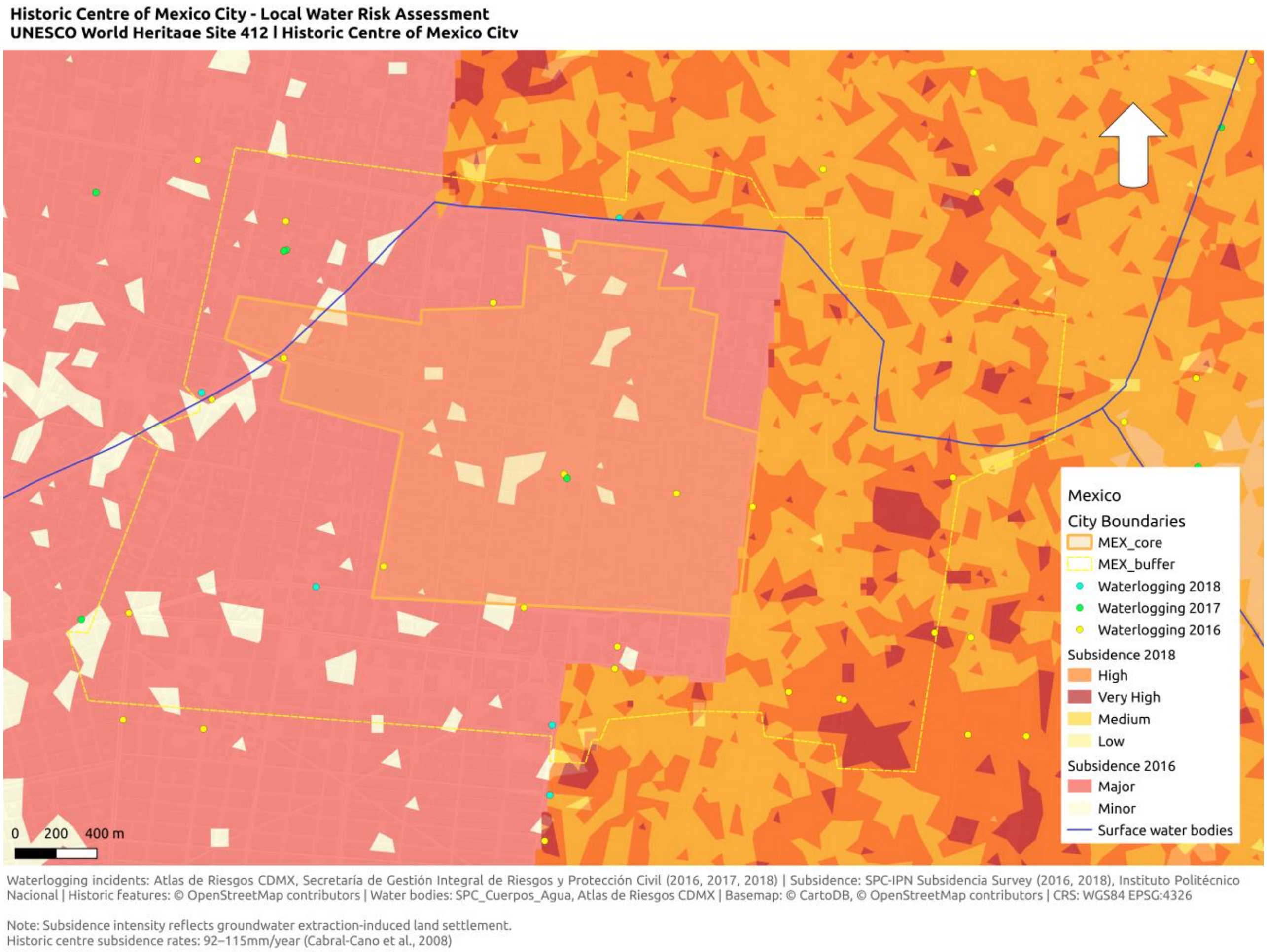

***Figure 16**: Historic Centre of Mexico City Local Water Risk Assessment.*

5.4 Tier 2 Summary: Site-Specific Risk Profiles

The Tier 2 local contextual analysis reveals that both sites face water-related risks operating through mechanisms that are invisible to the global datasets employed in Tier 1, and that are rooted in the interaction between urban water management practices and the underlying geological conditions of each heritage zone.

For Amsterdam, the primary risk is the bidirectional groundwater dependency of wooden pile foundations. Neither groundwater rise nor groundwater depletion is captured by the JRC flood hazard or surface water occurrence datasets, yet both constitute direct threats to the structural integrity of the 17th-century heritage fabric. The risk is not one of water arriving at the surface but of water behaving incorrectly below it, making conventional flood hazard modelling an inadequate tool for characterising Amsterdam's most critical conservation challenge.

For Mexico City, the primary risk is groundwater extraction-induced land subsidence, which threatens the structural integrity of historic buildings through differential settlement. Subsidence also has a secondary consequence for flooding: as the ground surface descends unevenly, the gradients that historically allowed surface water to drain away from the historic centre are disrupted, causing water to accumulate in areas that previously drained freely. The spatial coincidence of high and very high subsidence intensity zones (SPCIPN, 2018) with recurring waterlogging incident locations (SPC_Encharcamientos, 2016-2018) within and surrounding the WHS 412-001 boundary is consistent with this interpretation. The same areas that are sinking most severely are also the areas where surface water repeatedly accumulates after rainfall. The analysis does not directly measure drainage infrastructure condition, but the multi-year recurrence of waterlogging at consistent locations within high subsidence zones is spatially coherent with the argument that ground settlement is contributing to drainage failure. Direct measurement of drainage capacity degradation is recommended as a subject for future research.

In both cases, Amsterdam and Mexico, the most critical risk mechanism is subsurface rather than surface, confirming that global raster-based hazard datasets alone are insufficient for heritage water risk assessment at the site level and that local contextual analysis is not supplementary but essential to an accurate understanding of conservation risk.

The data asymmetry between the two cities is itself a finding of analytical significance. Amsterdam's mature, consistently maintained municipal GIS infrastructure contrasts with Mexico City's more heterogeneous multi-agency dataset landscape, reflecting differences in institutional capacity and open data governance rather than differences in the severity of risk. This asymmetry has direct implications for the UNESCO State of Conservation reporting framework: the capacity to monitor, document, and respond to water-related risks is unequally distributed across all World Heritage cities, and that inequality is not merely a data availability problem but a conservation governance challenge that warrants attention at the international heritage management level.

Nonetheless, this research demonstrates that meaningful localised risk analysis is achievable even where institutional data infrastructure is uneven. The Atlas de Riesgos CDMX, the SPC-IPN subsidence surveys, and the OpenStreetMap heritage asset data collectively enabled spatially explicit, multi-year analysis of subsidence intensity, waterlogging recurrence, and heritage exposure within the Mexico City Historic Centre, producing conclusions that are analytically comparable in depth and specificity to those derived from Amsterdam's purpose-built municipal datasets. The growing availability of open spatial data from national risk agencies, international research programmes, and community-contributed geographic databases means that heritage managers and researchers working in contexts with limited institutional GIS infrastructure are no longer without tools for site-level water risk assessment. What this research demonstrates is that the analytical framework matters as much as the data richness. A structured, tiered approach applied consistently across heterogeneous datasets can yield defensible spatial conclusions about heritage (water) risk regardless of the data landscape in which it operates.

6. CONCLUSION

6.1 Summary of Findings

This research set out to conduct a GIS-based evaluation of water-related risks to two UNESCO World Heritage Sites between 2020 and 2025, using the Amsterdam Canal Ring (WHS 1349) and the Historic Centre of Mexico City (WHS 412-001) as comparative case studies. Through a tiered analytical framework combining global raster datasets with city-specific local data, the research has produced a comparative spatial assessment of how water-related processes threaten Outstanding Universal Value across two culturally and hydrologically distinct heritage contexts.

The Tier 1 global comparative analysis demonstrated that both sites are characterised by high urban imperviousness and absence of meaningful surface water change over the 1984-2021 observation period, confirming that the dominant water risk mechanisms at both sites operate subsurface rather than through detectable surface hydrological change. The JRC flood hazard analysis revealed a fundamental divergence between the two sites: Amsterdam's heritage zone is excluded from the global flood model due to the effectiveness of its engineered flood defence infrastructure, while Mexico City's buffer zone records active modelled flood exposure under a 100-year return period scenario, with a mean depth of 0.68 metres and a maximum of 3.70 metres. This contrast reflects not only different hydrological geographies but different levels of investment in and effectiveness of water management infrastructure.

The Tier 2 local contextual analysis deepened this comparative picture by identifying the site-specific mechanisms through which water risk manifests at each heritage zone. For Amsterdam, the primary risk is the bidirectional groundwater dependency of the 17th-century wooden pile foundations, which are damaged by both groundwater rise and groundwater depletion. EGMS Level 3 SAR data confirmed consistent low-magnitude land subsidence across the inscribed boundary, with a mean vertical velocity of -0.85 mm/year across the core zone and greater spatial variability in the outer zone (mean -0.95 mm/year, min -3.64 mm/year). For Mexico City, the primary risk is groundwater extraction-induced land subsidence at rates of 92-115 mm/year, which threatens the structural integrity of historic buildings through differential settlement and compounds pluvial flood risk by disrupting urban drainage gradients. The spatial coincidence of high subsidence intensity zones with recurring waterlogging incident locations across the 2016-2018 Encharcamientos record provides spatial evidence consistent with this compounding mechanism.

The research also produced a methodological finding of significance beyond the two case studies. Despite the substantial asymmetry between Amsterdam's mature municipal GIS infrastructure and Mexico City's more heterogeneous multi-agency data landscape, meaningful site-level spatial analysis was achievable for both cities using openly available datasets. This demonstrates that the analytical framework: a structured, tiered approach applied consistently across heterogeneous data, matters as much as data richness, and that the growing ecosystem of open spatial data from national risk agencies, satellite programmes, and community-contributed databases has substantially reduced the barriers to heritage water risk assessment in data-sparse contexts.

This research makes two principal contributions to knowledge. The first is a contribution to Geographic Information Science: the development and demonstration of a transferable, open-source, tiered spatial analytical workflow for water risk assessment at World Heritage Sites. The workflow integrates globally consistent satellite-derived raster products, institutionally produced risk datasets, and community-contributed vector data within a structured zonal statistics framework, and was shown to produce meaningful spatial conclusions across two cities with substantially different data landscapes. The diversity of sources integrated, spanning satellite programmes from the European Commission, NASA, and ESA, national risk agencies in the Netherlands and Mexico, and municipal open data portals, demonstrates that the workflow is robust to data heterogeneity and replicable without proprietary tools or data. The inclusion of EGMS Level 3 SAR-derived ground motion data represents a methodological extension of the framework beyond surface flood hazard assessment into subsurface risk mechanisms, broadening its applicability to the full spectrum of water-related threats facing urban cultural heritage globally.

The second is a contribution to World Heritage risk science: the demonstration that the dominant water risk mechanisms at urban cultural heritage sites are subsurface rather than surface, and that they are invisible to the global raster datasets currently used as the primary evidence base for heritage flood risk assessment. At Amsterdam, the bidirectional groundwater dependency of 17th-century timber pile foundations constitutes a risk that no flood hazard model captures. At Mexico City, groundwater extraction-induced subsidence drives both structural damage and drainage failure in a self-reinforcing sequence that global surface water monitoring cannot detect. These findings make an empirical case for the integration of local contextual analysis, drawing on municipal risk datasets, SAR ground motion products, and site-specific heritage asset data, into the UNESCO State of Conservation monitoring framework as a necessary complement to global-scale assessments.

6.2 Responses to Research Questions

Research Question 1 asked what the prevalent water-related threats to World Heritage Sites globally between 2020 and 2025 are. The literature review identified fluvial flooding, pluvial flooding, groundwater rise and depletion, land subsidence, coastal inundation, erosion, waterlogging, and hydrological regime change as the principal categories of water-related threat. The case study analysis confirmed that pluvial flooding and groundwater-related mechanisms are the most analytically significant threats at both urban cultural heritage sites examined, consistent with the global literature's identification of these as the fastest-growing and most spatially pervasive water hazard categories.

Research Questions 2 and 3 asked how water events specifically impact natural and cultural heritage respectively. The case study analysis addressed the cultural heritage dimension through detailed local analysis at both sites. Natural heritage water risk was not the primary focus of this research, and its treatment is acknowledged as a limitation addressed in the Future Work section.

Research Question 4 asked how human settlement dynamics exacerbate or mitigate water-related threats. The analysis demonstrated that urban water management governance structure directly determines both risk exposure and monitoring capacity. Amsterdam's consolidated A3 management structure (Pereira Roders, 2010) enables integrated flood and groundwater management that effectively removes the heritage zone from global flood hazard models. Mexico City's fragmented A2 structure, combined with the legacy of the colonial drainage of Lake Texcoco and decades of uncontrolled groundwater extraction, has created a compounding risk environment in which urban water management practices are themselves the primary driver of heritage damage.

Research Questions 5 and 6 asked how GIS-based and remote sensing approaches can be effectively used for heritage water risk assessment. This research demonstrates that a structured spatial analytical framework applied consistently across heterogeneous, multi-source datasets can produce defensible, site-specific risk assessments for World Heritage properties. The Tier 1 analysis drew on globally consistent raster data products derived from satellite observation programmes spanning two continents and multiple data providers, including the JRC Global River Flood Hazard Maps (European Commission), the GMIS imperviousness dataset (NASA/CIESIN), and the JRC Global Surface Water suite (Pekel et al., 2016), each representing a distinct remote sensing methodology applied to a different dimension of water risk. The Tier 2 analysis incorporated pre-processed spatial analysis outputs and vectorised derivatives produced by national risk agencies, including the Atlas de Riesgos CDMX subsidence surveys (IPN/SGIRPC), the Amsterdam municipal flood probability model (KLIMAAT_OVERSTROMING), and the Rainproof groundwater risk zones, demonstrating that institutionally derived spatial analysis products can be integrated into a research framework alongside raw satellite rasters without loss of analytical rigour. The EGMS Level 3 ground motion data represents a further category of remote sensing product: a continental-scale InSAR-derived dataset pre-processed to annual mean velocity, enabling heritage managers to assess subsidence at inscribed properties across Europe without specialist interferometric processing capability. Together these datasets demonstrate that the barrier to entry for heritage water risk assessment using open spatial data has substantially decreased, and that the combination of globally consistent raster data products, nationally produced risk outputs, and community-contributed geographic data can sustain a multi-dimensional risk analysis at the site level.

6.3 Concluding Observations

This research confirms that water-related risks to World Heritage Sites are not adequately characterised by global flood hazard datasets alone. At both case study sites, the most critical risk mechanisms are subsurface rather than surface, driven by the interaction between urban water management practices and the underlying geological conditions of the heritage zone. Conventional global risk assessments that rely solely on fluvial flood modelling will systematically underestimate water risk at engineered urban heritage sites such as Amsterdam and will miss the dominant risk mechanisms at geologically complex sites such as Mexico City entirely.

The comparative approach adopted in this research reveals that water risk is not simply a function of hydrological exposure but of the relationship between heritage typology, urban governance structure, geological substrate, and management capacity. Two sites with broadly comparable global risk indicators can face profoundly different actual conservation challenges depending on the local conditions beneath and around them. This finding supports the argument for a tiered, locally grounded approach to heritage water risk assessment as a complement to global monitoring frameworks.

7. FUTURE WORK

This research has established a comparative baseline for water risk assessment at two urban World Heritage Sites and has identified several analytical directions that were beyond the scope of the current study but represent productive avenues for future research. Four principal directions are proposed.

7.1 Natural Heritage Water Risk Assessment

This research focused exclusively on cultural heritage. Future research should extend the tiered GIS framework to natural heritage contexts, where surface hydrological change is itself the primary risk indicator rather than a proxy for subsurface processes. Xochimilco (WHS 412-002), the co-inscribed component excluded from this analysis, represents an immediate extension. It's wetland system retains active surface water directly detectable by the JRC occurrence and seasonality layers, and the spatial overlap between urban encroachment and the surviving lacustrine landscape makes it an analytically appropriate next case

7.2 Quantitative Drainage and Outflow Analysis for Mexico City

This research demonstrated spatial coincidence between subsidence intensity and waterlogging recurrence but did not directly model drainage hydraulics. Future research should apply gradient analysis to the SPC_Corrientes_Agua drainage channel network using high-resolution elevation data and the SPC-IPN subsidence surface to identify channel reaches where differential subsidence has reversed or flattened outflow gradients below functional thresholds, directly quantifying drainage capacity loss attributable to ground settlement within WHS 412-001.

7.3 SAR-Based Ground Mechanics and Site-Specific Subsidence Analysis

The EGMS Level 3 annual mean velocity product used here provides zone-level characterisation of ground motion. Future research should apply time series analysis to individual persistent scatterer points within both heritage boundaries to reveal seasonal subsidence patterns driven by groundwater extraction cycles, acceleration trends, and spatial discontinuities indicating differential settlement between adjacent structures — enabling identification of specific buildings where subsidence is accelerating beyond the zone mean and warranting targeted structural assessment.

7.4 Site-Specific Heritage Asset Risk Analysis Using Spatial Intersection

The Tier 2 analysis confirmed risk coincidence at the zone level but did not rank individual assets. Future research should intersect heritage asset layers directly with risk surfaces to produce asset-level risk scores. For Amsterdam this means crossing Historic Buildings and Protected Trees with the Infiltration Capacity, Flood Model, and EGMS surfaces. For Mexico City it means crossing OSM historic building polygons with the SPC-IPN subsidence intensity and Encharcamientos waterlogging density.

REFERENCES

Journal Articles and Book Chapters

Arrighi, C. (2021). A global scale analysis of river flood risk of UNESCO World Heritage Sites. Frontiers in Water, 3, 764459. https://doi.org/10.3389/frwa.2021.764459

Bojorquez-Tapia, L. A., Cruz-Bello, G. M., Luna-Gonzalez, L., Juarez, L., and Ortiz-Perez, M. A. (2022). Water diversion in the Valley of Mexico Basin: An environmental transformation that caused the desiccation of Lake Texcoco. Land, 11(4), 542. https://doi.org/10.3390/land11040542

Cabral-Cano, E., Dixon, T. H., Miralles-Wilhelm, F., Diaz-Molina, O., Sanchez-Zamora, O., and Carande, R. E. (2008). Space geodetic imaging of rapid ground subsidence in Mexico City. Geological Society of America Bulletin, 120(11-12), 1556-1566. https://doi.org/10.1130/B26001.1

Chaussard, E., Havazli, E., Fattahi, H., Cabral-Cano, E., and Solano-Rojas, D. (2021). Over a century of sinking in Mexico City: No hope for significant elevation and storage capacity recovery. Journal of Geophysical Research: Solid Earth, 126, e2020JB020648. https://doi.org/10.1029/2020JB020648

Duffy, K., and Gavin, K. (2023). Opportunities and challenges of press-in piling for sustainable inner-city quay wall development in Amsterdam. Proceedings of the SAHC 2023 Conference, Delft University of Technology.

Farr, T. G., Rosen, P. A., Caro, E., Crippen, R., Duren, R., Hensley, S., Kobrick, M., Paller, M., Rodriguez, E., Roth, L., Seal, D., Shaffer, S., Shimada, J., Umland, J., Werner, M., Oskin, M., Burbank, D., and Alsdorf, D. (2007). The Shuttle Radar Topography Mission. Reviews of Geophysics, 45, RG2004. https://doi.org/10.1029/2005RG000183

Ginzarly, M., Joshi, M. Y., and Teller, J. (2024). A multidimensional framework for assessing cultural heritage vulnerability to flood hazards. International Journal of Heritage Studies, 30(10), 1173-1192. https://doi.org/10.1080/13527258.2024.2378438

Katontoka, M., Noardo, F., Palacios-Lopez, D., Esch, T., Nourian, P., Chen, F., and Pereira Roders, A. (2024). No report, no densification? A spatiotemporal analysis of urban densification and reporting practices in World Heritage properties. Land, 13(10), 1646. https://doi.org/10.3390/land13101646

Klaassen, R. K. W. M., Creemers, G., and Hamelink, M. (2023). Rate of occurrence of wood degradation in foundations and archaeological sites when groundwater levels are too low. Journal of Cultural Heritage, 63, 1-12. https://doi.org/10.1016/j.culher.2023.07.009

Li, M. (2024). Disaster risk management of cultural heritage: A global scale analysis of characteristics, multiple hazards, lessons learned from historical disasters, and issues in current DRR measures in world heritage sites. International Journal of Disaster Risk Reduction, 110, 104633. https://doi.org/10.1016/j.ijdrr.2024.104633

Nguyen, K. N., and Baker, S. (2023). Climate change and UNESCO World Heritage-listed cultural properties: A systematic review, 2008-2021. Heritage, 6(3), 2394-2420. https://doi.org/10.3390/heritage6030126

Ortega, A. (1989). The groundwater regime of the Valley of Mexico from historic evidence and field observations. Journal of Hydrology, 112(3-4), 171-190. https://doi.org/10.1016/0022-1694(89)90187-9

Pekel, J. F., Cottam, A., Gorelick, N., and Belward, A. S. (2016). High-resolution mapping of global surface water and its long-term changes. Nature, 540, 418-422. https://doi.org/10.1038/nature20584

Valagussa, A., Frattini, P., Crosta, G., Spizzichino, D., Leoni, G., and Margottini, C. (2021). Multi-risk analysis on European cultural and natural UNESCO heritage sites. Natural Hazards, 105(3), 2659-2676. https://doi.org/10.1007/s11069-020-04417-7

Reports, Conference Proceedings, and Institutional Publications

Aylett, L., Montagna, M., Murai, M., and Badman, T. (2025). IUCN World Heritage Outlook 4. IUCN. https://doi.org/10.2305/NYKJ7099

CLIMAAX. (2024). Hazard assessment for river flooding using flood maps. CLIMAAX Climate Risk Assessment Handbook. Deltares / VU Amsterdam. https://handbook.climaax.eu/notebooks/workflows/FLOODS/02_River_flooding/Hazard_assessment_FLOOD_RIVER.html

Deltares. (2024). Foundations on wooden piles: Groundwater sensitivity and decay mechanisms. Deltares Technical Report.

Pereira Roders, A. (2010). Revealing the World Heritage cities and their varied natures. In Proceedings of the 3rd International Conference on Heritage and Sustainable Development (Heritage 2010). Eindhoven University of Technology.

Pereira Roders, A., Loes, V., Rianne, B., and Michael, T. (2015, December). Human settlements managing World Heritage: Results of a global survey (1978-2015). UNESCO World Heritage Centre.

TU Delft. (2023). Assessment and long-term performance of timber pile foundations in the Netherlands. Delft University of Technology Repository.

UNESCO and Heritage Governance Sources

UNESCO World Heritage Centre. (1987). Nomination dossier: Historic Centre of Mexico City and Xochimilco (WHS 412). UNESCO. https://whc.unesco.org/en/list/412

UNESCO World Heritage Centre. (1997). Mill Network at Kinderdijk-Elshout (WHS 818). UNESCO. https://whc.unesco.org/en/list/818

UNESCO World Heritage Centre. (2010). Nomination dossier: Seventeenth-Century Canal Ring Area of Amsterdam inside the Singelgracht (WHS 1349). UNESCO. https://whc.unesco.org/en/list/1349

UNESCO World Heritage Centre. (2026). Outstanding Universal Value. UNESCO. https://whc.unesco.org/en/glossary/327

UNESCO World Heritage Cities Programme. (2025). Historic building and heritage boundary layers — Amsterdam [dataset]. UNESCO / ArcGIS Urban Heritage Atlas. Feature service including WHS boundary polygons (Middeleeuws stadshart 1012 and Amsterdam-Binnen de Singelgracht) and historic building point data. https://services6.arcgis.com/eMd5K6XXEvJETxfQ/arcgis/rest/services/Historic_Building/FeatureServer

Spatial Datasets

Atlas de Riesgos CDMX. (2016, 2017, 2018). SPC_Encharcamientos [dataset]. Secretaria de Gestion Integral de Riesgos y Proteccion Civil (SGIRPC), Ciudad de Mexico. https://www.atlas.cdmx.gob.mx/datosabiertos.html

Atlas de Riesgos CDMX. (2016). SPC_IPN_Subsidencia_2016 [dataset]. Instituto Politecnico Nacional / SGIRPC, Ciudad de Mexico. https://www.atlas.cdmx.gob.mx/datosabiertos.html

Atlas de Riesgos CDMX. (2018). SPC_Subsidencia_IPN_CII-III-IV_2018 [dataset]. Instituto Politecnico Nacional / SGIRPC, Ciudad de Mexico. https://www.atlas.cdmx.gob.mx/datosabiertos.html

Baugh, C., Colonese, J., D'Angelo, C., Dottori, F., Neal, J., Prudhomme, C., and Salamon, P. (2024). Global river flood hazard maps - 100-year return period [dataset]. European Commission Joint Research Centre (JRC). https://data.jrc.ec.europa.eu/collection/id-0054

Center for International Earth Science Information Network (CIESIN), Columbia University. (2022). Global Man-made Impervious Surface (GMIS) Dataset from Landsat, v1 (2010) [dataset]. NASA Socioeconomic Data and Applications Center (SEDAC). https://www.earthdata.nasa.gov/data/catalog/sedac-ciesin-sedac-ulandsat-gmis-v1-1.0.

European Environment Agency / Copernicus Land Monitoring Service. (2024). European Ground Motion Service Level 3 (EGMS L3) - Mean velocity 2020-2024 [dataset]. ESA Copernicus. https://land.copernicus.eu/en/products/european-ground-motion-service/ Accessed May 2026.

Gemeente Amsterdam. (2024). BOMEN_BIJZONDER (Protected Trees) [dataset]. Amsterdam Open Geodata Portal. https://maps.amsterdam.nl/open_geodata/?k=561/ Accessed May 2026.

Gemeente Amsterdam. (2024). BHISTORISCHE_BEBOUWING (Heritage Buildings) [dataset]. Amsterdam Open Geodata Portal. https://maps.amsterdam.nl/open_geodata/?k=118/ Accessed May 2026.

Gemeente Amsterdam. (2024). KLIMAAT_OVERSTROMING (Climate Flood Model) [dataset]. Amsterdam Open Geodata Portal. https://maps.amsterdam.nl/open_geodata/?k=318/ Accessed May 2026.

Gemeente Amsterdam. (2024). RAINPROOF_DRAINAGE (Infiltration Capacity) [dataset]. Amsterdam Open Geodata Portal. https://maps.amsterdam.nl/open_geodata/?k=290/ Accessed May 2026.

JRC Global Surface Water Explorer. (2021). Global Surface Water dataset - Occurrence, Seasonality layers [dataset]. European Commission Joint Research Centre (JRC). https://global-surface-water.appspot.com/download/ Accessed May 2026.

Baugh, C., Colonese, J., D'Angelo, C., Dottori, F., Neal, J., Prudhomme, C., & Salamon, P. (2024). *Modelled flood inundation for different return period scenarios at the global scale* [Dataset]. European Commission, Joint Research Centre (JRC). https://jeodpp.jrc.ec.europa.eu/ftp/jrc-opendata/CEMS-GLOFAS/flood_hazard/ Accessed May 2026.

OpenStreetMap contributors. (2024). OpenStreetMap [dataset]. OpenStreetMap Foundation. https://www.openstreetmap.org

OpenTopography. (2015). Shuttle Radar Topography Mission (SRTM) GL1 — 30m resolution [dataset]. Distributed by OpenTopography. https://portal.opentopography.org/raster?opentopoID=OTSRTM.082015.4326.1 Accessed May 2026.

Basemaps and Web Sources

Decolonial Atlas. (2018, May 12). Mexico City's buried history [map]. Jordan Engel. https://decolonialatlas.wordpress.com/2018/05/12/mexico-citys-buried-history/

Esri. (2024). World Imagery [basemap]. Esri, DigitalGlobe, GeoEye, Earthstar Geographics, CNES/Airbus DS, USDA, USGS, AeroGRID, IGN, and the GIS User Community. https://server.arcgisonline.com/ArcGIS/rest/services/World_Imagery/MapServer

Waternet. (2024). Groundwater in Amsterdam. Waternet Municipal Water Authority. https://www.waternet.nl/en/our-water/groundwater/ Accessed May 2026.

Waternet. (2024). Water management in Amsterdam. Waternet Municipal Water Authority. https://www.waternet.nl/en/ Accessed May 2026.

APPENDICES

Appendix A: UNESCO Nomination File Boundary Maps for the Case Study Cities

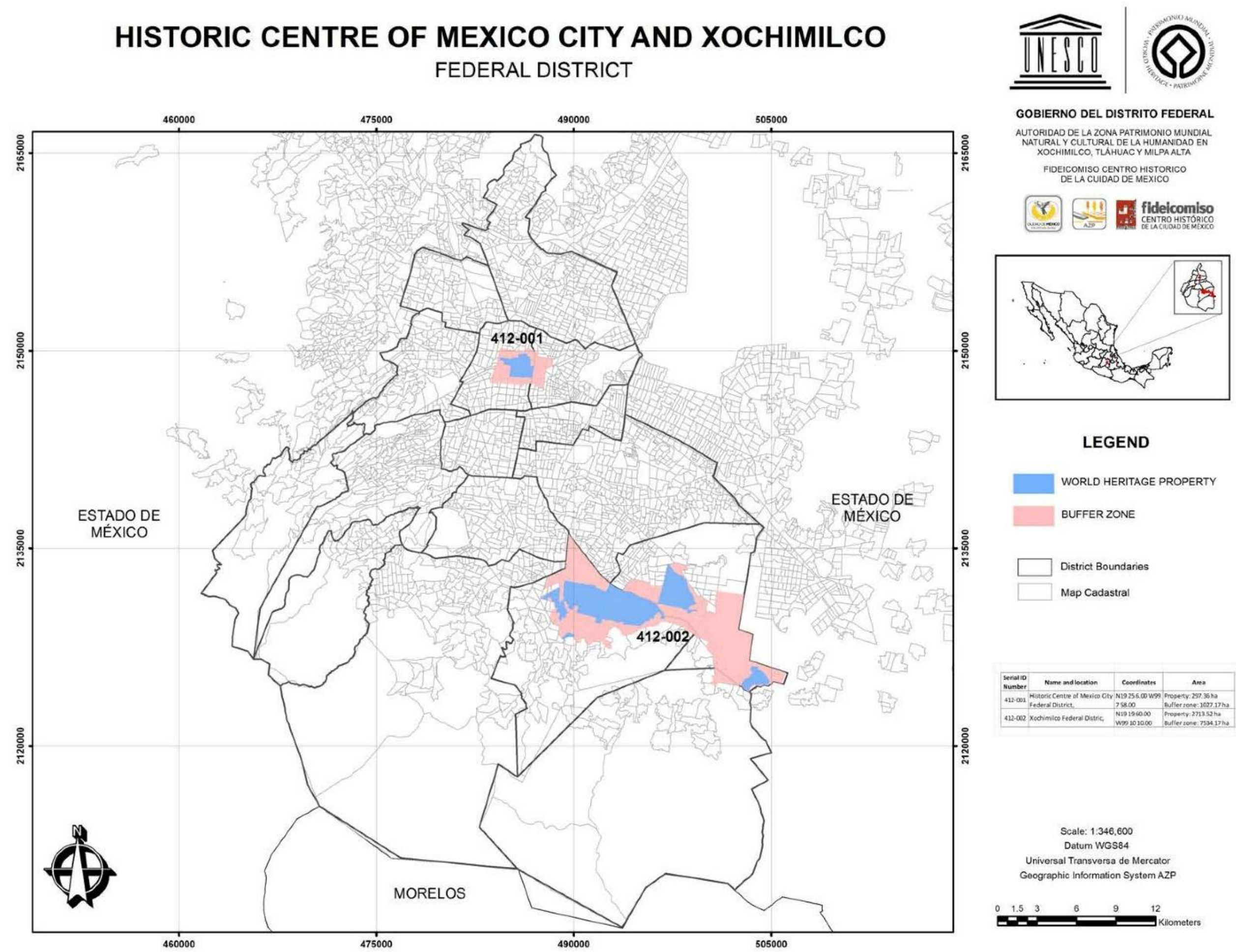

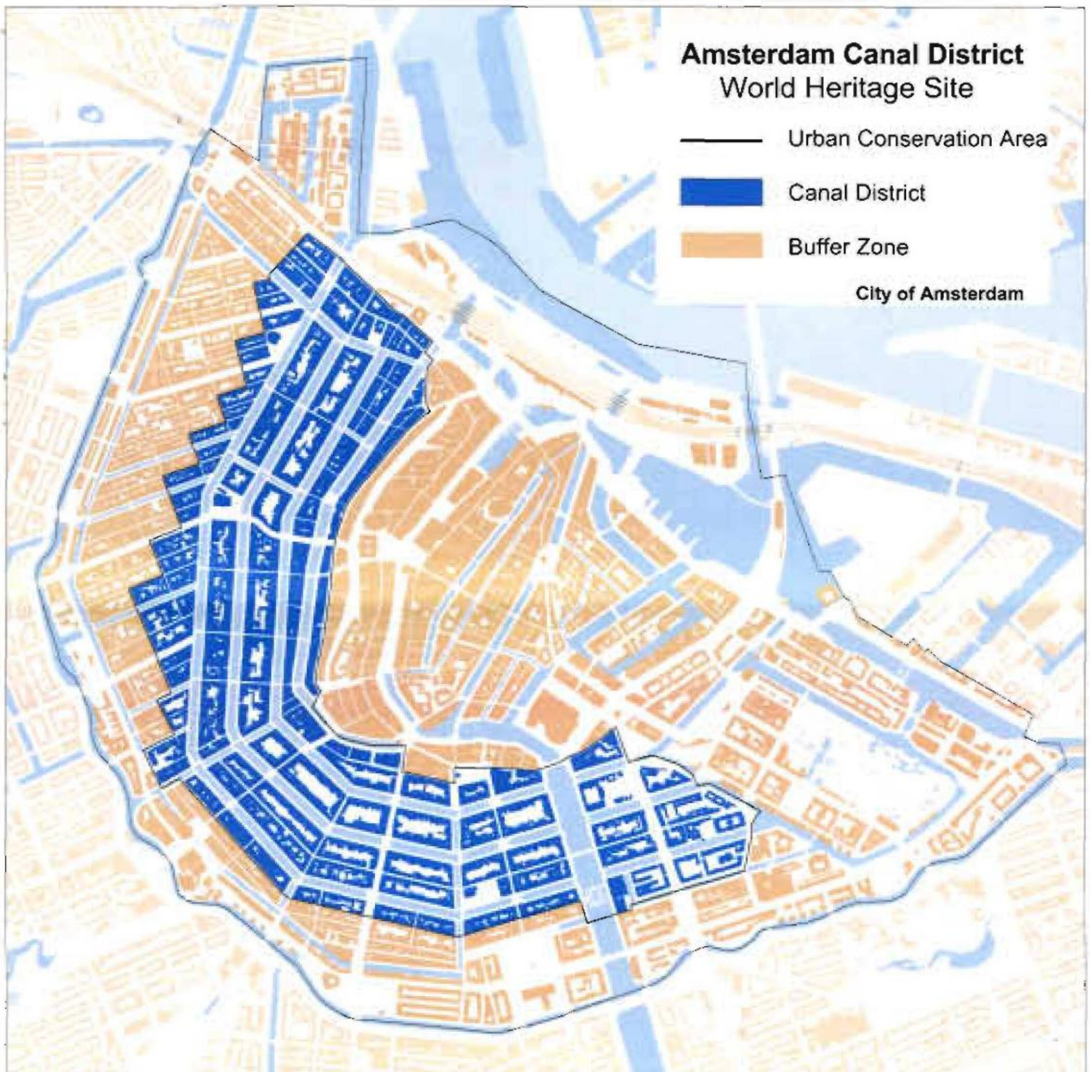

Amsterdam Canal District
World Heritage Site
Urban Conservation Area
Canal District
Buffer Zone
City of Amsterdam

Appendix B: Batch Zonal Statistics Python Script

The following Python script was executed within the QGIS 3.22 Python console to compute zonal statistics for all raster layers across all four polygon zones in a single automated batch operation. The script processes each polygon-raster combination, saves outputs as GeoPackage files, loads them into the QGIS project, and prints a full summary table to the console. The script is designed for reproducibility and can be adapted for other study areas by updating the file paths and polygon/raster dictionaries.

File: WHS_zonal_statistics.py | Language: Python 3 | Environment: QGIS 3.22 Python Console

```
"""
WHS Water Risk — Batch Zonal Statistics

Runs zonal statistics for all raster layers against all polygon zones
(AMS_core, AMS_buffer, MEX_core, MEX_buffer) and saves outputs as .gpkg

"""

import os
from qgis.core import (QgsVectorLayer, QgsProject)
import processing

# FILE PATHS
INPUT_DIR  = "/home/dleoni/Downloads/WHS_Project"
OUTPUT_DIR = "/home/dleoni/Downloads/WHS_Project/zonal_outputs"

# POLYGON LAYERS
POLYGONS = {
    "AMS_core":   os.path.join(INPUT_DIR, "AMS_core.geojson"),
    "AMS_buffer": os.path.join(INPUT_DIR, "AMS_buffer.geojson"),
    "MEX_core":   os.path.join(INPUT_DIR, "MEX_core.geojson"),
    "MEX_buffer": os.path.join(INPUT_DIR, "MEX_buffer.geojson"),
}

# RASTER LAYERS — separate sets per city
RASTERS_AMS = {
    "flood":           os.path.join(INPUT_DIR, "AMS_flood.tif"),
    "gmis":            os.path.join(INPUT_DIR, "AMS_gmis.tif"),
    "swoccurrence":    os.path.join(INPUT_DIR, "AMS_occurrence.tif"),
    "seasonality":     os.path.join(INPUT_DIR, "AMS_seasonality.tif"),
    "changeintensity": os.path.join(INPUT_DIR, "AMS_changeintensity.tif"),
}
RASTERS_MEX = {
    "flood":           os.path.join(INPUT_DIR, "MEX_flood.tif"),
    "gmis":            os.path.join(INPUT_DIR, "MEX_gmis.tif"),
    "swoccurrence":    os.path.join(INPUT_DIR, "MEX_occurrence.tif"),
    "seasonality":     os.path.join(INPUT_DIR, "MEX_seasonality.tif"),
    "changeintensity": os.path.join(INPUT_DIR, "MEX_changeintensity.tif"),
}
POLYGON_RASTER_MAP = {
    "AMS_core":   RASTERS_AMS,
    "AMS_buffer": RASTERS_AMS,
    "MEX_core":   RASTERS_MEX,
    "MEX_buffer": RASTERS_MEX,
}

# STATISTICS: Mean(2), Min(5), Max(6), Majority(9) — QGIS 3.22 codes
STATS = [2, 5, 6, 9]

if not os.path.exists(OUTPUT_DIR):
    os.makedirs(OUTPUT_DIR)

results_summary = {}

for poly_name, poly_path in POLYGONS.items():
    print(f"\n{'='*50}")
    print(f"Processing polygon: {poly_name}")
    if not os.path.exists(poly_path):
        print(f"  WARNING: Polygon not found: {poly_path}")
        continue
    results_summary[poly_name] = {}
    rasters = POLYGON_RASTER_MAP[poly_name]
```

```
    for raster_name, raster_path in rasters.items():
        if not os.path.exists(raster_path):
            print(f"  WARNING: Raster not found: {raster_path}")
            continue
        print(f"  Running: {poly_name} x {raster_name}")
        output_name = f"{poly_name}_zonal_{raster_name}"
        output_path = os.path.join(OUTPUT_DIR, f"{output_name}.gpkg")

        result = processing.run("native:zonalstatisticsfb", {
            'INPUT':        poly_path,
            'INPUT_RASTER': raster_path,
            'RASTER_BAND':  1,
            'COLUMN_PREFIX': f"{raster_name}_",
            'STATISTICS':   STATS,
            'OUTPUT':       output_path
        })

        layer = QgsVectorLayer(output_path, output_name, "ogr")
        if layer.isValid():
            QgsProject.instance().addMapLayer(layer)
            f = list(layer.getFeatures())[0]
            fields = [fld.name() for fld in layer.fields()]
            def get_val(suffix):
                for fn in fields:
                    if fn.endswith(suffix): return f[fn]
                return "NULL"
            mean = get_val("_mean"); mn = get_val("_min")
            mx   = get_val("_max");  maj = get_val("_majority")
            print(f"    Mean: {mean}  Min: {mn}  Max: {mx}  Majority: {maj}")
            results_summary[poly_name][raster_name] = {
                "mean": mean, "min": mn, "max": mx, "majority": maj
            }

# PRINT SUMMARY TABLE
print(f"\n{'='*70}")
print("FULL RESULTS SUMMARY")
print(f"{'='*70}")
for poly_name, rasters in results_summary.items():
    print(f"\n{poly_name}:")
    print(f"  {'Raster':<20} {'Mean':<12} {'Min':<12} {'Max':<12} {'Majority':<12}")
    print(f"  {'-'*60}")
    for rn, s in rasters.items():
        print(f"  {rn:<20} {str(s['mean']):<12} {str(s['min']):<12} {str(s['max']):<12}
{str(s['majority']):<12}")
print(f"\nBatch zonal statistics complete.")
print(f"Outputs saved to: {OUTPUT_DIR}")
```

Zonal Statistics Console Output

The following output was produced by running the batch script above against the final corrected dataset, using the official Amsterdam heritage boundaries (Rijksbeschermd stadsgezicht, Gemeente Amsterdam) and the georeferenced UNESCO 412-001 boundary for Mexico City. This output represents the final accepted zonal statistics results used in Table 4 and throughout the Tier 1 results analysis.

Execution environment: QGIS 3.22 Python Console | Date: May 2nd, 2026 | CRS: WGS84 EPSG:4326

```
==================================================
Processing polygon: AMS_core
==================================================
  flood        Mean: 1.0     Min: 1.0     Max: 1.0     Majority: 1.0
               [Note: uniform value 1.0 = JRC classified zone code, not depth in metres]
  gmis         Mean: 70.864  Min: 0.0     Max: 200.0   Majority: 100.0
  swoccurrence Mean: 1.402   Min: 0.0     Max: 97.0    Majority: 0.0
  seasonality  Mean: 0.224   Min: 0.0     Max: 12.0    Majority: 0.0
  changeintens Mean: 249.202 Min: 0.0     Max: 254.0   Majority: 253.0

==================================================
Processing polygon: AMS_buffer
==================================================
  flood        Mean: 1.0     Min: 1.0     Max: 1.0     Majority: 1.0
               [Note: uniform value 1.0 = JRC classified zone code, not depth in metres]
  gmis         Mean: 81.673  Min: 0.0     Max: 200.0   Majority: 100.0
  swoccurrence Mean: 6.584   Min: 0.0     Max: 99.0    Majority: 0.0
  seasonality  Mean: 0.997   Min: 0.0     Max: 12.0    Majority: 0.0
  changeintens Mean: 239.686 Min: 0.0     Max: 254.0   Majority: 253.0

==================================================
Processing polygon: MEX_core
==================================================
  flood        Mean: NULL    Min: NULL    Max: NULL    Majority: NULL
               [Note: NULL = no JRC modelled flood data within inscribed boundary]
  gmis         Mean: 90.202  Min: 5.0     Max: 100.0   Majority: 100.0
  swoccurrence Mean: 0.0     Min: 0.0     Max: 0.0     Majority: 0.0
  seasonality  Mean: 0.0     Min: 0.0     Max: 0.0     Majority: 0.0
  changeintens Mean: 253.0   Min: 253.0   Max: 253.0   Majority: 253.0

==================================================
Processing polygon: MEX_buffer
==================================================
  flood        Mean: 0.684   Min: 0.126   Max: 1.558   Majority: 0.370
  gmis         Mean: 85.826  Min: 0.0     Max: 100.0   Majority: 100.0
  swoccurrence Mean: 0.002   Min: 0.0     Max: 25.0    Majority: 0.0
  seasonality  Mean: 0.001   Min: 0.0     Max: 8.0     Majority: 0.0
  changeintens Mean: 252.995 Min: 200.0   Max: 253.0   Majority: 253.0

======================================================================
FULL RESULTS SUMMARY
======================================================================

AMS_core:
  Raster               Mean         Min          Max          Majority
  ------------------------------------------------------------
  flood                1.0          1.0          1.0          1.0
  gmis                 70.864       0.0          200.0        100.0
  swoccurrence         1.402        0.0          97.0         0.0
  seasonality          0.224        0.0          12.0         0.0
  changeintensity      249.202      0.0          254.0        253.0

AMS_buffer:
  Raster               Mean         Min          Max          Majority
  ------------------------------------------------------------
  flood                1.0          1.0          1.0          1.0
  gmis                 81.673       0.0          200.0        100.0
  swoccurrence         6.584        0.0          99.0         0.0
  seasonality          0.997        0.0          12.0         0.0
  changeintensity      239.686      0.0          254.0        253.0

MEX_core:
  Raster               Mean         Min          Max          Majority
  ------------------------------------------------------------
```

```
  flood                NULL         NULL         NULL         NULL
  gmis                 90.202       5.0          100.0        100.0
  swoccurrence         0.0          0.0          0.0          0.0
  seasonality          0.0          0.0          0.0          0.0
  changeintensity      253.0        253.0        253.0        253.0

MEX_buffer:
  Raster               Mean         Min          Max          Majority
  ------------------------------------------------------------
  flood                0.684        0.126        1.558        0.370
  gmis                 85.826       0.0          100.0        100.0
  swoccurrence         0.002        0.0          25.0         0.0
  seasonality          0.001        0.0          8.0          0.0
  changeintensity      252.995      200.0        253.0        253.0

======================================================================
Batch zonal statistics complete.
Outputs saved to: /home/dleoni/Downloads/WHS_Project/zonal_outputs
======================================================================
```